

*The structure of planktonic communities
under variable coastal upwelling conditions
off Cape Ghir (31°N), in the Canary Current
System (NW Africa)*

Presentado

Por:

Valeria Anabalón Molina

Tutores :

Javier Arístegui Ruiz

Carmen Morales Van de Wyngard

UNIVERSIDAD DE LAS PALMAS DE GRAN CANARIA

Programa de Oceanografía

Las Palmas de Gran Canaria, España

2013

ÍNDICE

1. ABSTRACT.....	2
2. Introduction and objectives	3
3. Materials and Methods.....	5
4. Results.....	9
5. Discussion.....	15
6. Conclusions.....	22
7. Acknowledgements.....	23
8. References.....	23
9. Figure legends.....	33
10.Figures.....	35
11.Tables.....	47

ABSTRACT.-

Cape Ghir ($\sim 31^{\circ}\text{N}$), in the Canary Current System, is an area of permanent coastal upwelling with maximum intensity in summer-autumn, when a stronger across-shore thermal gradient and increased mesoscale activity are also present. The effects of spatial (a coastal-ocean transect with 7 stations) and temporal (5 dates: from December 2008 to October 2009) variations in upwelling conditions on the structure of planktonic communities was investigated. Multivariate analyses on the environmental conditions identified two main upwelling phases, weak and moderate; additionally, the most coastal station was, in all cases, distinct from the rest. Cluster formation was mostly influenced by nutrient concentration (space), and by sea surface temperature and number of days favourable to upwelling (time). These clusters were also representative of the spatial and temporal variability in the planktonic assemblages, implying that changes in the upwelling conditions do influence community structure. In terms of biomass, the dominant functional groups were mixed assemblages of dinoflagellates and ciliates (>51%); diatoms contributions were moderate to low (<35%) and their

space and time variability was comparatively lower. The biomass in size fractions was dominated by the microplankton (>53%), which was mostly represented by dinoflagellates and ciliates. As autotrophic biomass, total chlorophyll-a was dominated by the nanoplankton fraction (flagellate and dinoflagellate); however, diatoms and dinoflagellates (microplanktonic) made the highest contributions to carbon biomass. This paradox probably results from suboptimal physiological conditions for diatoms and/or from a significant contribution by mixotrophs (microplanktonic dinoflagellate and ciliate taxa). Mean heterotrophic:autotrophic biomass ratios (pico-to microplankton) were mostly ≤ 1 (normal pyramid) when the contribution of mixotrophs was considered but >1 (inverted pyramid) without it. The factors that might contribute to the structure of the phytoplankton assemblages in this system most likely include nutrient limitation in the upwelled waters, a narrow continental shelf, mesoscale activity dominated by the formation of a strong across-shore front and of a weak filament, and wind intensities which are mostly weak to moderate for most of the year.

Introduction

The coastal waters off NW Africa in the Canary Current System (CCS; 10-33°N) are among the most productive in the world in terms of pelagic and demersal resources (Arístegui et al., 2005, 2009; Chavez and Messié, 2009), sustained by the upwelling of cold, higher nutrient waters in the coastal band which stimulate high

levels of primary production (up to $5 \text{ g C m}^{-2} \text{ d}^{-1}$) and of phytoplankton biomass (up to $10 \text{ mg chlorophyll-a m}^{-3}$) (Van Camp et al., 1991; Freudenthal et al. 2001a; Lauthuilere et al., 2008; Arístegui et al., 2005, 2009). Coastal upwelling processes in the CCS are favoured by the dominance of trade winds (NE direction). The latitudinal shift of the Azores subtropical high-pressure system and of the tropical deep-pressure system related to the Intertropical Convergence Zone (ITCZ) generate temporal variations in intensity of upwelling (Barton et al., 1998; Pelegrí et al., 2005a). In addition, other features (e.g. bathymetry, coastal geometry, and topography) contribute to strengthen the coastal upwelling processes, especially in the areas around capes. At least 3 main upwelling areas have been identified in this region (Marcello et al., 2011): between Cape Ghir and C. Juby ($25\text{--}33^\circ\text{N}$); from C. Bojador to C. Blanc ($20\text{--}25^\circ\text{N}$); and around C. Vert ($12\text{--}20^\circ\text{N}$).

The area off Cape Ghir ($\sim 31^\circ\text{N}$) is characterized by the presence of a submarine plateau, which extends offshore (150 km from the coast), being a branch of the Atlas Mountains (Hagen et al., 1996; Barton et al., 1998). This region displays high mesoscale activity, including the formation of fronts, eddies and filaments in the coastal transition zone (Hagen et al., 1996; Hernandez-Guerra & Nykjaer, 1997; Barton et al., 1998; Nieto et al., 2012). In particular, a recurrent filament (C. Ghir filament) has been detected, having a highly variable length (from 30 to 300 Km) (Hagen et al., 1996; Hernandez-Guerra & Nykjaer, 1997; Barton et al., 1998). North of C. Ghir, a high positive wind stress curl is also recurrent and it has been attributed to the orographic influence of the Atlas Mountains and the concave shape of the coastline just south of C. Ghir (Hagen et al., 1996). All these features stimulate considerable temporal and spatial variability in the oceanographic conditions in this area (Van Camp et al., 1991; Zhao et al., 2000; Sicre et al., 2001). However, studies describing in detail the dynamics of coastal upwelling and mesoscale structures in the

area off C. Ghir are still few and sporadic in time and space (Van Camp et al., 1991; Hagen et al., 1996; Nykjaer and Van Camp, 1994; Freudenthal et al., 2001a, 2002). Only recently, the variability in upwelling conditions over this area, and the whole of the CCS, has been analyzed using a 20-year time series on winds and surface temperature (Marcello et al., 2011); also, the mesoscale frontal and filament variability has been analyzed in detail for this system using high resolution surface temperature data (Nieto et al., 2012). Altogether, these studies indicate that upwelling off C. Ghir is almost permanent, with peaks during summer and fall associated with a strengthening of the upwelling favourable wind and results in a stronger coastal-ocean gradient in sea surface temperature (SST).

The effects of upwelling processes and mesoscale features on the pelagic ecosystem in the area off Cape Ghir have been assessed mostly in terms of organic matter export and chlorophyll-a (Chl-a) distribution (Head et al., 1996; Neuer et al., 2002; Freudenthal et al., 2001a, 2002; Arístegui & Harrison 2002; García-Muñoz et al., 2005; Pelegrí et al. 2005, 2005b). Most of these studies have been of very short duration and with little detail on the structure of the planktonic communities. In areas adjacent to C. Ghir, like the Canary Islands, the spatio-temporal variability in the structure of planktonic communities in the coastal upwelling and coastal transition zones has been addressed by several authors (Hagen et al., 1996; Barton et al., 1998; Arístegui et al., 2002, 2004, 2005, 2009; Baltar et al., 2009). These studies have shown that variations in the intensity of upwelling winds and in the water column stratification strongly influence the structure of phytoplankton communities as well as primary production. However, these results have focused only on one or two plankton size fractions within the range of the phytoplankton components (pico- to microplankton). Only one study covered the complete range of phytoplankton size classes, but was focused in the area of the filament off C. Juby (Arístegui et al., 2004).

Moreover, the sampling time was short (2 consecutive weeks) and did not include estimates of carbon biomass for each size or functional group, nor a detailed taxonomic composition of the organisms.

Based on the available knowledge, the question posed here is whether the spatial and temporal variations in the coastal upwelling conditions off Cape Ghir produce significant changes in the structure of the planktonic communities in the coastal band and the adjacent coastal transition zone. In line with the results for other upwelling areas in the CCS (Aristegui et al., 2004, 2005; Baltar et al., 2009) and other coastal upwelling systems (Chavez et al., 2009; Morales et al., 2007; Gonzalez et al., 2007; Kudela et al., 2005, 2010; Crespo et al., 2012; Espinoza et al., 2012), we expected to find that periods of intense upwelling would favour the dominance of diatoms in the nearshore area, where the maxima in nutrient concentrations is usually found. In contrast, periods of weak upwelling would benefit the increase of nanoplanktonic of flagellated forms, together with a more homogeneous distribution of plankton abundance and biomass in the coast-ocean direction. In these terms, this study evaluates the effects of variations in upwelling conditions, in its spatial (coastal-ocean) and temporal (intra-annual) dimensions, on the structure of the planktonic communities in the coastal upwelling and coastal transition zones off C. Ghir. The structure of the communities was analyzed in terms of size (from pico- to microplankton) and functional groups (eg Flagellates, Dinoflagellates, Diatoms, Cyanobacteria), as well as with regard to the dominant taxa within these groups.

2. Materials and Methods

2.1. Study area, oceanographic samples, and complementary satellite data

A total of 5 cruises were conducted off Cape Ghir (December 2008, and February, June, August, and October 2009) on board the Moroccan R/V “Amir Moulay Abdellah (AMA)”, from the INRH (4 cruises), and the Spanish R/V “Sarmiento de Gamboa” (August 2009), from the Spanish Research Council (CSIC), in the frame of the CAIBEX project. During each cruise, a transect perpendicular to the coast (31°N) was sampled, including 7 stations from the coast (9.8°W) to 150 km offshore (11.2°W). The most coastal station (E1) was located at ~2.3 km from the coast (30 m depth); the stations were ~10-17 km apart closer to the coast (E1-E5) whereas those located farther offshore (E5-E7) were ~30-34 km apart (Fig. 1a).

Hydrographic data were obtained with a CTD Sea Bird SBE-9-11 equipped with a fluorescence sensor (WetStar). Temperature and salinity data were used to estimate water density (as $\sigma\text{-t}$) and stratification intensity ($J\text{ m}^{-3}$) according to Bowden (1983). Discrete seawater samples were collected with Niskin bottles (5 L) for the analyses of macro-nutrients (PO_4 , SiO_2 , NO_2 , and NO_3) and Chl-a (total, and 2 size fractions: $<20\ \mu\text{m}$ and $<3\ \mu\text{m}$). Five depth levels (0, 25, DCM (depth of Chl-a maximum fluorescence), 90 and 150 m depth) were considered, except in the most shallower stations (E1: 0, 10, and 25 m; and E2: 0, 10, 25, 50, 75 or 90 m). Chl-a samples were analyzed by the fluorometric method (Holm-Hansen et al., 1965), with a Turner Designs 10AU fluorometer; nutrients were analyzed with a Technicon-Bran Luebbe AAI analyzer, following JGOFS recommendations (UNESCO, 1994).

Satellite data on winds, sea level, sea surface temperatures (SST), and Chl-a were analyzed to provide a wider coverage of the spatial and temporal dimension during which the in situ observations took place. Daily wind data ($1/4^\circ$ spatial resolution) were derived from the combined product CCMP (Cross-Calibrated Multi-Platform

Ocean Surface Wind Vector) L3.0, from the Physical Oceanography Distributed Active Archive Center (PO.DAAC; <ftp://podaac-ftp.jpl.nasa.gov>). CCMP contains intercalibrated wind measurements of the following missions: SSM/I, SSMIS, AMSR-E, TRMM TMI, QuikSCAT, SeaWinds, and WindSat. Wind stress and the number of days favourable to upwelling prior to the cruise were estimated from these data. Daily SST data (AVHRR Pathfinder V5.0) were obtained from NOAA (<ftp://data.nodc.noaa.gov/pub/data.nodc/Pathfinder>) at a 2x2 Km grid resolution. Sea level anomaly (SLA) data were obtained from the combined processing of TOPEX/JASON (1/4° x 1/4° resolution) from the ERS altimeter, distributed by AVISO (<http://aviso.oceanos.com>); the geostrophic velocity field was estimated from SLA. Daily satellite images of Chl-a were derived from HERMES, a product of combined sensors (MODIS, MERIS, SeaWiFS), obtained from GlobColorWeb (<ftp.fr-acri.com> or <http://hermes.acri.fr/>).

2.2. Plankton community structure: composition, abundance and biomass

Plankton samples at the same depth levels as for nutrients and Chl-a were obtained directly from the Niskin bottles, transferred to amber glass bottles (250 mL), and immediately preserved with an acid Lugol's solution (2% final concentration), following the Utermöhl method (Villafañe and Reid, 1995). Nanoplankton (2-20 µm) and microplankton (20-200 µm) were analyzed with an inverted microscope (ZEISS AXIOVERT 35) with 1000x resolution. The enumeration lasted until at least 200 cells (nanoplankton) or 100 cells (microplankton) of the dominant taxa were registered in each sample. The following guides were used for taxonomic identification: Tomas, 1997; Ojeda, 1998; Anderson et al. 2002; Lynn and Small, 2002; Thompson, 2004.

Nanoplankton samples were also analyzed by epifluorescence to distinguish the cells according to their trophic function (autotrophs/mixotrophs or heterotrophs).

Water samples were transferred to 50 mL tubes and immediately preserved with glutaraldehyde (1% final concentration; Gifford and Caron, 2000), and stored under cold (~4°C) and dark conditions. Within 5 days after the sampling date (except in June 2009, when there was a delay of 3 months), subsamples of 20 mL (0-50 m depth) or 50 mL (90-150 m depth) were stained with a mixture of DAPI (4,6-diamidino-2-phenylindole) and Proflavine (3-6 diamino-acridine hemi-sulfate) at a final concentration of 5 $\mu\text{g mL}^{-1}$ (Verity and Sieracki, 1993), and then vacuum-filtered (<10 mm Hg) onto black polycarbonate membrane filters (0.6 μm pore, 25 mm diameter). These filters were immediately mounted on glass slides and a drop of immersion oil was added before covering them with a glass cover slip; they were then stored at -20°C in darkness until subsequent analysis (<8 months). Nanoplankton was enumerated (1000x magnification) with an epifluorescence microscope (ZEISS AXIOVERT 35) equipped with a digital camera plus UV (385-400 nm), blue (450-480 nm) and green (480-550 nm) filters. The enumeration included at least 100 cells of the most dominant taxa in each sample.

Picoplankton (0.2-2 μm) was enumerated by flow-cytometry (Becton-Dickinson FACScalibur with 488 nm argon ion laser). Duplicate samples were collected in sterile cryovials (2 mL), immediately fixed with glutaraldehyde (0.1% final concentration), and frozen in liquid nitrogen (-196°C) in darkness until analysis (Marie et al., 2000). For the enumeration of picoheterotrophs (bacterioplankton), the samples were stained with SYTO-13 (Molecular Probes Inc.), using a dilution of the stock solution (1:10) to a final concentration of 2.5 μM ; their signature was identified in a plot of side scatter (SSC) versus the green fluorescence (FL1). The identification and enumeration of picoautotrophs (*Prochlorococcus*, *Synechococcus*, and picoeukaryotes) in unstained samples was based on the analysis of multiple bivariate scatter plots of SSC, and red and orange fluorescences. The analyses were run at low

speed for the bacterioplankton and at medium or high speed for the picoautotrophs, until 10,000 events were acquired. A suspension of yellow-green 1 μm latex beads (10^5 and 10^6 mL beads mL^{-1} for picoautotrophs and bacterioplankton, respectively) was added as an internal standard (Polyscience Inc). The flow rate was determined volumetrically after every 10 samples run.

Plankton C-biomass was obtained from cell volume estimates for representative taxa in the different functional groups; volume measurements were taken during each of the cruises considering that cell size of a given taxa can display large variations (see Supplementary Table 1). For nano- and microplanktonic cells, geometric models were applied (Balech, 1948; Chrzanowski and Simek, 1990; Alder, 1999; Sun and Lui, 2003). At least 20 cells of each type/taxa were randomly selected and measured using a micrometer grid as a reference; median values were obtained for each case. The following carbon/biovolume conversion factors in the literature were used after a preliminary evaluation which indicated that they provided the most conservative estimates: Menden-Deuer and Lessard (2000) for ciliates, dinoflagellates, and diatoms; Heinbokel (1978) for Tintinnids; and Børsheim and Bratbak (1987) for Flagellates. Also, a correction for biovolume estimates for the Lugol-fixed samples (microplankton) was applied, following Choi and Stoecker (1989). For the picoplankton, the following conversion factors were applied: 29 fg C cell^{-1} for *Prochlorococcus* and 100 fg C cell^{-1} for *Synechococcus* (Zubkov et al., 2000), and 1.5 pg C cell^{-1} for picoeukaryotes (Zubkov et al., 1998). Bacterioplankton biomass was estimated assuming a conversion factor of 12 fg C cell^{-1} (Fukuda et al., 1998).

The proportion between heterotrophic (H) and autotrophic (A) biomasses (H:A ratios), as an indicator of the trophic structure of communities in the oceans (Gasol et al., 1997), was also estimated. Flow-cytometry and epifluorescence allowed the distinction of the trophic function in the picoplankton and nanoplankton, respectively,

but in the case of the microplanktonic this was derived from the literature as applied to specific taxa. Mixotrophy was not directly evaluated though it is common in dinoflagellates and ciliates (eg Stoecker et al., 1987; Bernard and Rassoulzadegan, 1994; Jacobson and Anderson, 1994; Kang et al., 2010; Jeong et al., 2010) but all cells with natural fluorescence were identified as autotrophs in the case of the pico- and nanoplankton. In the case of microplanktonic dinoflagellates and ciliates which have been identified as mixotrophic species/genera in the literature, the approach of Stoecker et al. (1987, 1989, 1996) and Bernard and Rassoulzadegan (1994) was applied and by which 40% of the total biomass of mixotrophs is allocated to the autotrophic biomass. The H:A biomass ratios obtained with and without this correction were compared. Also, C:Chl-a were obtained.

2.3 Statistical analyses of data

All statistical analyses (either uni- or multivariate) of the biological data were carried out using integrated values (see Table 2); depth has a strong influence on plankton distribution but the main focus of this study is on the horizontal and temporal variation (comparisons with non-integrated data were included in some cases as to evaluate the influence of depth). For the environmental variables, surface (temperature and salinity) and integrated (nutrients) data were used, in addition to the following data: wind stress (W), the number of days with winds favourable to upwelling prior to each cruise (WD), and the inshore-offshore SST gradient. Chl-a was not included in the multivariate analyses but its variation was analyzed separately with a non-parametric 2-way (spatial and temporal dimensions) ANOVA (Kruskal-Wallis), since the data displayed non-normality and/or non-homogeneity of variance (Kolmogorov-Smirnov and Browne Forsythe tests; Zar, 1984).

Multivariate analyses were performed with the PRIME software v.6 (Clarke and Warwick, 2001; Clarke and Gorley, 2006) to explore the spatial and temporal

variations in the structure of the planktonic communities, as well as their association with the environmental conditions. Data were transformed in the environmental matrix ($\log n+1$) and the biological matrix (square root) to normalize them and to avoid asymmetry between the two matrices. In applying community similarity analyses, the Euclidean distance was used for the environmental variables and Bray-Curtis for the biological data. The spatial and temporal variations in the environmental and biological data were analyzed separately with the CLUSTER (hierarchical clustering) and MDS (non-metric multi-dimensional scaling) routines; the significance of the clusters was verified with the SIMPROF (similarity profile) routine. The ANOSIM (analysis of similarities) and SIMPER (species contributions) routines were used to assess the similarities and the dissimilarities between clusters with respect to the temporal and spatial variability in the biological matrix (at the level of functional groups and genera/morphological types). The associations between the biological data and the environmental variables were analyzed with the BIO-ENV and RELATE routines. In turn, the best combinations of variables determined by BIO-ENV were subjected to further analysis (LINKTREE) to determine the variable(s) which best represented the separation of the biological components into different groups/clusters.

3. Results

3.1. Variability of satellite-derived wind, SST and Chl-a

Satellite time series data (June 2008-December 2009) of wind stress, SST and Chl-a, covering the field-sampling region off Cape Ghir, were processed. A predominance of wind upwelling favourable conditions was observed (Fig. 1b); some unfavourable

events occurred during winter months (December-February) whereas events of relative relaxation were present during the fall (September-October). The SST distribution (Fig. 1c) displayed a seasonal pattern, with colder waters in winter-spring (December to June) and warmer in summer-autumn months (June to December). Also, the SST gradient along the sampling transect (9.8 -11.2°W) was lower during the winter-spring period (higher across-shore homogeneity). In terms of Chl-a (Fig. 1d), the highest values ($>2 \text{ mg m}^{-3}$) were registered nearer to the coast ($<25 \text{ km}$ from the coast) throughout the period; extensions further offshore of such values were detected during the summer-autumn period and during short events in winter.

The satellite-derived distributions of wind velocity and direction, SST and Chl-a in the region between 30 and 32° N during the sampling dates (Fig. 2) were in agreement with those observed in the satellite time series for the area off Cape Ghir (Fig. 1b-d). The average wind speeds (Fig. 2, left panels) were moderate to high ($4\text{-}10 \text{ m s}^{-1}$) and favourable to upwelling during all the samplings, except in Jun-09. During the winter samplings, the average SST values (Fig. 2, center panel) were lower and had a nearly homogeneous spatial distribution whereas during the summer-autumn samplings, the lower SST were restricted to the inshore and a strong thermal gradient between the coasta and the ocean was evident; in Jun-09, this gradient was mostly N-S in direction (Table 1). In addition, mesoscale structures were observed, as derived from the geostrophic velocity field and SST distribution. A filament (sensu Van Camp et al., 1991; Peligrí et al 2005) was detectable during the Aug-09 and Oct-09 samplings; jets, meanders, and eddies were also present during some of the samplings (Fig. 2 central and right panels). In terms of Chl-a (Fig. 2, right panels), the highest values ($\geq 1 \text{ mg m}^{-3}$) were mostly concentrated near the coast but intermediate values ($0.5\text{-}1 \text{ mg m}^{-3}$) extended offshore during winter (mainly during Feb-09).

3.2. Variability of in situ oceanographic conditions and Chl-a distribution

Temperatures between 14 and 20°C, and salinities between 36.0 and 36.6, in the water column during the field sampling were indicative of the presence of North Atlantic Central West Water (NACW); density was dominated by variations in temperature (Fig. 3). Temperature-salinity diagrams (Fig. 3) confirmed that the water column structure during winter was more homogeneous, both horizontally and vertically (0-200 m depth), in comparison to the summer-autumn samplings when stronger stratification occurred (Table 1).

A preliminary analysis of data on wind direction and intensity (Fig. 2), the ascent of the 26.7 kg m⁻³ isopycnal in the coastal zone (Fig. 3), and the SST gradient (Table 1) during the field sampling allowed us to distinguish the following phases: weak upwelling (WEKUP: Dec-08 and Feb-09), relaxation (RELAX: Jun-09), and moderate upwelling (MOUP: Aug-09 and Oct-09). A 2-way ANOSIM analysis revealed significant environmental variability between stations (coastal and coastal transition) and upwelling phases ($r = 0.52$, $P = 0.001$), except between RELAX and MOUP ($r = 0.008$, $P = 0.41$). In concordance with this, CLUSTER and MDS analyses identified the following clusters (Fig. 4): A) the most coastal station (E1), a result of the shallowness of this station, and B) which contains 2 different upwelling phases: WEKUP phase (cluster C) and MOUP phase (cluster D); the RELAX phase represented a transition between the WEKUP and MOUP phases (SIMPROF, $P_i = 0.42$, $P = 0.001$). The variables that contributed most to the separation of these clusters (SIMPER analysis) were: a) nutrient concentration (SiO₂, PO₄ and NO₃): WEKUP vs. E1 (similarity distance = 30), b) nutrient concentration (SiO₂, PO₄) and SST: MOUP vs. E1 (s. distance = 30), and c) water density, SST and the number of days which were favourable to upwelling (WD): WEKUP vs. MOUP (s. distance = 15).

Total Chl-a (Fig. 5, left panels), representing the biomass of autotrophs/mixotrophs, showed a similar pattern of distribution as the satellite-derived data (Fig. 2). The distributions of Chl-a in the nano- and picoplankton size fractions (Fig. 5, right central and right panels) were significantly different between the 3 clusters described above (Kruskal-Wallis, $n = 35$, $p < 0.05$), but not for the microplankton (Fig. 5 left central panels). The contribution of the nanoplankton to total Chl-a was moderate but mostly high (30-93%) during the samplings, with a maximum at coastal stations during RELAX and MOUP (Oct-09) phases. Microplankton Chl-a was highly variable (2-85%), mostly lower than the contribution of the nanoplankton and with maxima at the most coastal stations during contrasting phases. The contribution of the picoplankton fraction to total Chl-a was mostly in the low range (<25%) but during the Aug-09 sampling it was similar to that of the nanoplankton fractions whereas that of the microplankton was at its minimum (Table 1).

3.3. Structure of the planktonic communities

The following nano-and microplankton components (as functional groups, taxa and/or types) were identified during the sampling period 160 samples): (a) 43 diatom (DIAT) genera (size range: 10-200 μm); (b) 27 dinoflagellate (DIN) genera (8-150 μm); (c) 32 ciliate (CIL) genera (15-150 μm); (d) 8 flagellate (FL) genera and 6 morphotypes, mostly in the nanoplankton size range but 4 of them were colonial (20-80 μm); and e) 2 silicoflagellate (SIL) genera. A small number of coccolithophores were found in some samples but were not included in the analysis since the preservation technique applied was not appropriate for this group (Table 2).

Cell abundance in the nanoplankton (Fig. 6) was dominated by nanoflagellates (NFL) and, secondarily (an order of magnitude lower), by nanodinoflagellates (NDIN). The contribution of the autotrophic/mixotrophic NFL represented >80% of

all NFL, as was the case for NDIN, except in Feb-09 when it was <40%. In the microplankton (Fig.7), cell abundance was dominated by microdiatoms (MDIAT), followed by colonial flagellates (MFL) and microdinoflagellates (MDIN). The nanoplankton and the microplankton were concentrated in the upper 50 m depth. The relative contributions to total abundance and carbon (C) biomass (as integrated values) of different taxa and size categories in the nano-and micro-plankton fractions are represented in Fig. 8 (as percentages) and detailed in Table 3 (as absolute values). As size fractions, the nanoplankton accounted for the largest proportion (80-95%) of the total abundance during the samplings whereas the microplankton contributed most to the total biomass (43-99%) but 20 to 57% of it was provided by the nanoplankton (Fig. 8a-b). MDIAT were the main contributors to the total abundance in the microplankton fraction during 3 different phases; in contrast, during Dec-08, the MFL contributed with 50% of the total whereas in Aug-09, the MDIN were dominant (Fig. 8c). In terms of biomass, the contributions of MDIN and MCIL were the largest, except in Jun-09 (Fig. 8d). The NFL were the largest contributors to total abundance in the nanoplankton fraction (Fig. 8e); their biomass was lower during MOUP, when that of NDIN increased whereas during RELAX both were similar (Fig. 8f).

In the picoplankton, data were available only for 3 samplings. The integrated abundance and biomass of HB and APP are represented in Fig. 9. The HB accounted for the largest proportion of the total picoplankton abundance (91-99%), with a maximum during Dec-08 whereas the contribution to biomass was moderate to high (19-59%). The contribution of APP to picoplanktonic biomass was moderate to high (41-81%) despite its low relative abundance (1-9%). The cyanobacteria (CIAN: PRO and SYN) contributed the most (65-84%) to total APP abundance whereas PEU made similar or greater contributions to APP biomass during Feb-09 and Aug-09 (54-89%); the biomasses of SYN and PEU were similar during Dec-08. Biomass changes in the

APP components (Table 3) were well represented by Chl-a in that size fraction (Fig. 5, right panels), with a maximum in Aug-09 and a minimum in Feb-09.

3.4. Temporal and spatial variability of the plankton under varying upwelling intensity

Depth-integrated abundance and biomass of the nano- and microplanktonic components (as functional groups, taxa and/or morphotypes) were significantly different between phases and sampling stations (2-way ANOSIM, $r = 0.7$, $P = 0.001$; $r = 0.37$, $P = 0.004$, respectively), as reflected in the MDS and cluster analyses. In terms of abundance (Fig. 10a), the main groups or clusters identified were coincident with those detected for the environmental variables: A) the most coastal Station (E1) and B) which contains different upwelling phases: WEKUP (cluster C) and MOUP + RELAX (cluster D). For the biomass (Fig. 10b), the same 2 clusters were identified (A and B); in this case, however, B was subdivided in 3 clusters representing the different phases (MOUP, WEKUP C, and RELAX). The separation into these clusters was significant in both cases (SIMPROF, $P_i \geq 4.32$, $P = 0.001$). The analysis of dissimilarity between these groups (SIMPER) indicated that, in terms of abundance, FL was the functional group which most contributed to the separation of the clusters, with moderate percentages from DIAT and DIN (Tables 4 and 5). At more specific level, the greatest contributions to dissimilarity were provided by NFL as a size fraction (NFL-1 in particular) and the Gymnodiniaceae (DIN) at the family level (mostly by *Gymnodinium* spp.), followed by Bacillariaceae (DIAT). In terms of biomass, the functional groups, which contributed most to dissimilarity, were DIN in the first place, followed by DIAT and CIL. At a more specific level, the most important contributors were again, the Gymmodiniaceae, followed by Ceratiaceae (DIN) and Strombidiidae (CIL). The inclusion of the picoplankton fraction (only 3 sampling) in the SIMPER analyses influenced the above results but only moderately

in terms of abundance and minimal in terms of biomass (Tables 4 and 5).

The functional group, which primarily contributed to the dissimilarity, were the FL (35%; greater WEKUP) and, secondarily, DIAT (25%) and DIN (23%). However, DIAT did contributed the most (35%) to the dissimilarity between the coastal (E2, E3, E4) and the coastal transition stations (E5, E6, E7), with secondary contributions from FL (29%) and DIN (24%).

A correlation analysis between the biological components (as integrated abundance and biomass of the nano- and microplankton fractions) and the spatio-temporal variations in upwelling conditions was significant (RELATE, $r \geq 0.51$, $P < 0.001$). The environmental variables that best explained the changes in the biological components (BIO-ENV) were a combination of SST and integrated NO₃ and PO₄ for the abundance ($r = 0.77$, $P < 0.001$); and WD, integrated NO₃ and PO₄, and SS for the biomass ($r = 0.70$, $P < 0.001$). The variables that best defined the separation between the biological components into the clusters described above (Fig. 11) were as follows (LINKTREE): Group A (St. E1) vs. the rest of stations (Group B) – nutrient concentration in terms of abundance and biomass. For abundance alone (Fig. 11a), SST was decisive in the division of group B into 4 subgroups (B', C, D, G) which included different upwelling phases and distances from the coast; for biomass alone (Fig. 11b), WD best separated the groups in B. When the picoplankton data were included in these analyses (only 3 samplings), the patterns were very similar (RELATE, $r \geq 0.81$, $P < 0.001$), with WD and integrated NO₃ and PO₄ best explaining the changes in abundance and biomass (BIO-ENV: $r = 0.89$; $P < 0.001$). LINKTREE results also showed the same trends: group A (St. E1) separation from the rest (group B) was explained by nutrients for both abundance and biomass; group B formed 2 groups, MOUP (Aug-09) and WEKUP (Dec-08 and Feb-09) phases which were best explained by changes in WD (Table 6).

3.5. Other community descriptors and their spatio-temporal variability

The contributions of autotrophic (A) and heterotrophic (H) components to total C-biomass (all corrected for mixotrophy) were estimated for all the stations and samplings, together with the H:A ratios including all size fractions (pico- to microplankton) for the 3 samplings (Dec-08, Feb-09, and Aug-09) which included these components (Table 3). The relative contribution of APP ranged between 14 and 25% of the total autotrophic biomass, with a maximum in Dec-08; CIAN contribution was small (2-3%) compared to that of PEU (11-23%). The average (between stations of one sampling) contribution of autotrophic FL (AFL: 8-25%), which includes mostly nanoflagellates but also silicoflagellates and micro-flagellates for this purpose, was also larger in Dec-08 when comparing the 3 samplings; it ranged between 5% (Jun-09) and 21% (Oct-09) during the other samplings which did not include the picoplankton. The average contribution of the DIAT (15-38%), which were mostly in the microplankton fraction, was larger during Feb-09 when comparing the 3 samplings and attained 33-40% in the remaining 2 samplings; that of auto/mixotrophic (ADIN) ranged between 22 and 37% for the 3 samplings, being largest in Aug-09, and 23 and 36% (Jun-09 and Oct-09, respectively) in the remaining samplings. The CIL, which were mostly represented in the microplankton fraction, contributed with <20% in most samplings, except during the Oct-09 sampling (25%). Overall, the autotrophic biomass of the communities during the samplings was composed mostly by DIAT and ADIN (60-69%), except in Dec-08 when the contributions of APP, AFL, and ADIN were dominant.

In terms of the heterotrophic C-biomass, the HB contributed between 11 and 31% of the total (maximum in Dec-08) whereas the heterotrophic FL (HFL) in the nanoplankton size range, represented a very small proportion (<2%) when comparing

the 3 samplings, as above. In contrast, the heterotrophic/mixotrophic DIN (HDIN) and CII (HCIL) made the largest contributions during those 3 samplings (30-66% and 22-39%, respectively) as well as during the other 2 samplings 53-76% and 23-46%, respectively). Total H:A biomass ratios (H:A) were >1.5 during the 3 samplings which included the whole planktonic community (Table 3), when no correction for mixotrophy was applied. However, after correcting for it in the case of MDIN and MCIL, these ratios (Hm:Am) diminished (≤ 1.0), being lowest during the WEKUP phase (Dec-08 and Feb-09). That is, the correction for mixotrophy applied to the microplankton, together with the relative large contribution of this size fraction to total C-biomass, made a significant change in the biomass distribution of the communities (from inverted to normal pyramids).

In addition, the contributions of the different size fractions to total autotrophic C-biomass (A) and Chl-a biomass were estimated in terms of the A:Chl-a ratios (Table 3). As a total autotrophic community, including from pico- to microautotrophs, the A:Chl-a ratios ranged between 50 and 64 and the correction for mixotrophy (Am:Chl-a) slightly increased these values ($<20\%$); in the 2 samplings which only had the nano- and microautotrophs, these values were 29 and 78 and slightly higher than those after the correction for mixotrophy. The A:Chl-a ratios were highly variable between size fractions and samplings (14-450); the correction for mixotrophy in the microplankton (MATm) fraction increased the ratios to different extent but to 100% in Dec-08. The relationship between C-biomass and Chl-a was also analyzed by linear regression (Table 7); as total and by size fractions, the relationships were significant, except for the microplankton when no correction for mixotrophy was applied. In addition, different trophic groups were significantly related: HB and total Chl-a, MHT and total Chl-a, and HB and NHT (Table 7).

4. Discussion

4.1. Oceanographic, nutrient and Chla-a variability in the area off Cape Ghir

Wind conditions and SST distribution in the area around Cape Ghir during this study (June 2008–November 2009; Fig. 1 b-c) were similar to those described previously for this area, with predominant northeast winds favourable to upwelling during most of the year and a strong seasonality in the cross-shelf SST gradient which is at its maximum during the summer and autumn (Barton et al., 1998; Arístegui et al., 2006, 2009; Pelegri et al., 2005a, 2005b; Lathuiliere et al., 2008). Using data from a long time-series, Marcello et al. (2011) concluded that the whole of the coastal band between 20 and 33°N off NW Africa is characterized by persistent upwelling, being more intense during summer and autumn in the area between 25 and 33°N. Despite the recurrence of upwelling in this region, as well as in similar coastal upwelling systems located in subtropical regions (Mackas et al., 2006), the changes in the oceanographic conditions are significant within the annual cycle and, probably, at smaller time scales. Our results have shown that this variability included, at least, two distinct phases, WEKUP and MOUP. The phase change was represented by variations in: a) the direction, duration, and intensity of the winds favourable to upwelling, b) the strength of the SST cross-shelf gradient, and c) the degree of water column stratification; a transition between these two phases was the RELAX condition (Fig. 3). Strong upwelling conditions (mean wind stress values higher than -0.2 N m^{-2} for several days) were not registered during our samplings but they were present during April and July 2009 (Fig. 1b). In fact, sampling due to be carried out during April 2009 was cancelled because of the strong winds.

The variability in upwelling conditions off Cape Ghir was also significant in the spatial dimension, where the most coastal station (E1) was markedly different from

the other stations along the cross-shelf transect, regardless of the stage of upwelling (Figs. 10-11). This variability was mainly attributed to differences in the across-shore nutrient concentration; though the integrated nutrients were lower in E1 because of a considerably lower depth of integration compared with the rest (Table 1; Fig. 11), the reverse was true when comparing the integrated nutrients in the surface 25 m layer (Fig. 12). This difference may be explained by the presence of a narrower continental shelf in the area between Casablanca (33°30'N) and C. Ghir, and/or the formation of a strong thermal front (as well as filaments) which attain its maximum expression between June and November (summer-autumn), in association with maximum upwelling intensity (Nieto et al., 2012). During our samplings, the thermal front was stronger during the MOUP phase, as it was the offshore extension of an upwelling plume (it was not strictly a cold filament, based on the velocity field; Fig. 2); nevertheless, the highest nutrient concentrations decreased considerably offshore of the most coastal station during all the samplings and, therefore, these two features do not contribute to explain such difference.

At the regional level, the nitrate content of the surface layer in the northern area of the CCS (24-33°N), which includes C. Ghir, is comparatively lower than in the southern area (15-23°N; Arístegui et al., 2006; Lathuiliere et al., 2008). Moreover, conditions of nutrient limitation for phytoplankton growth has been recently proposed for the northern part but not for the southern area (Lachkar & Gruber, 2012). Overall, the northern part of the CCS has nutrient concentrations which are considerably lower in comparison with other coastal upwelling systems, such as the Humboldt Current System (Thiel et al., 2007; Morales & Anabalón, 2012), the California Current System (Oram et al., 2008; Keister et al., 2009a), and the Benguela System (Shannon et al., 1985; Hutchings et al., 2009). In summary, the combination of a narrow shelf, low nutrient content in the upwelled waters, and weak to moderate upwelling

intensities, might explain the spatial zonation of nutrients off C. Ghir, having a narrow coastal upwelling zone (eutrophic conditions) and a very close to shore coastal transition zone (mesotrophic to oligotrophic conditions).

The intensity of upwelling winds, shelf width, nutrient content in upwelled waters, as well as mesoscale activity and the presence of fronts, are all factors which influence Chl-a concentration and its distribution in coastal upwelling areas (Lathuiliere et al., 2008; Chavez & Messié, 2009; Lachkar & Gruber, 2012). Our results indicate that there was significant variability in the offshore distribution of total Chl-a concentration during the annual cycle but, in general, the highest values were restricted to the first 25 to 50 km from the coast (Fig. 1d; Table 1), as it has been previously reported for this area (Garcia-Muñoz et al., 2005; Lathuilière et al., 2008), and in concordance with a narrow distribution of the higher nutrient levels (Fig. 12). The extension offshore of high Chl-a values was mostly explained by eddies, meanders, and an upwelling plume during this study (Fig. 2). Also, our results show that the size fraction which contributed the most to total Chl-a values, as average per sampling, was the nanophytoplankton (Table 2), regardless of the upwelling phase. In contrast, other studies in the surrounding coastal areas have shown a strong seasonal pattern in Chl-a, including a dominance of microphytoplankton during late winter - early spring, nanoplankton in autumn, and picophytoplankton in summer (Aristegui & Montero, 2005; Pelegri et al., 2005b; Baltar et al., 2009).

The average concentrations of in situ Chl-a during the different samplings varied within a relatively low range (35-81 mg m⁻²) but the differences between stations during different samplings ranged between orders of magnitude (8-232 mg m⁻²; Table 2). Previous Chl-a data off C. Ghir and C. Juby (Garcia-Muñoz et al., 2005; Pelegri et al., 2005b, Aristegui et al., 2004) have also shown relatively small changes in integrated Chl-a (11-90 mg m⁻²) compared to that in primary production (0-4.2 g C m⁻²

$^2 \text{ day}^{-1}$). Based on these differences in magnitude, Aristegui et al. (2004) proposed that phytoplankton biomass was consumer-controlled whereas primary production was resource-controlled; our results, however, suggest that phytoplankton biomass is resource-controlled (bottom-up control) in the area off C. Ghir. Recently, Lachkar & Gruber (2012) have proposed that net primary production in the northern region of the CCS appears to be resource-controlled but that the eco-physiological characteristics of the dominant functional groups or species compensate for it. In these terms, our results on community structure should be helpful in unveiling the composition of such dominant functional groups.

4.2. Plankton community structure under semi-permanent upwelling: the system off Cape Ghir

Planktonic communities in coastal upwelling systems are subject to strong oceanographic variability over a wide range of temporal and spatial scales (Shannon et al., 1985; Largier et al., 1993). Most studies on these communities have focused primarily on the variability in the phytoplanktonic and, mostly, the microplanktonic components during the annual cycle, and have generally concluded that diatoms dominate during the spring-summer period when upwelling develops (seasonal upwelling systems) or is more intense (permanent upwelling systems), shifting to dinoflagellates towards the end of summer and early fall, when water column stratification increases (Margalef 1978; Hutchings et al. 1995; Kudela et al., 2005). Smaller phytoplankton size fractions have more recently been recognized as important components in coastal upwelling systems (eg Aristegui et al., 2004; Sherr & Sherr, 2006; Bottjer & Morales, 2007, Espinoza et al. 2012, Crespo et al. 2012) although Probyn (1992) had established earlier their dominance in the Benguela system.

However, the spatial and temporal variability in the size structure of phytoplankton (and microbial components in general) and on their relative contribution to total C-biomass in the CCS is almost unknown (Aristegui et al., 2004, 2005).

In systems with permanent or semi-permanent coastal upwelling, such as areas of NW Africa (20-33°N), N Chile (18-30°S), California (24-32°N) and Benguela (18-28°S), a dominance of diatoms during periods of higher upwelling intensity and in the most coastal area has been detected (Aristegui et al., 2004, 2005; Herrera & Escribano, 2006; Freon et al., 2009). Our results, however, showed that a maximum in diatoms, as integrated abundance and biomass, occurred during dissimilar upwelling phases (Fig. 9, Table 2), suggesting that the intensity of upwelling was not the main factor explaining these maxima. Temporal and/or spatial variations in the nutrient content of the upwelled waters are an alternative; the average N:Si ratio (water-column and between stations) was close to 1 (1.3-1.6 mol/mol) during Feb-09, Jun-09, and Oct-09 whereas it was higher (>2.0 mol/mol) and, therefore, Si-limiting, during the rest. Coincident with this, the maximum in mean diatom abundance (across the transect) occurred during those 3 samplings of no Si-limitation; in terms of C-biomass, this group was lowest in Dec-08 but comparatively not so much in Aug-09 (Table 2). A limitation by Si in diatom assemblages was previously described for this area (Treguer & Le Corre 1978, Fanning 1992) and for surrounding areas (Voituriez & Le Borgne, 1974; Romero et al., 2002), therefore, Si-limitation could be the most important factor explaining the lack of diatom dominance in the study area, except at the most coastal stations during Jun-09 and Oct-09 (Figs. 7).

The abundance and biomass of dinoflagellates did show a clear association with the upwelling phase (maxima during RELAX and MOUP; Figs. 7-8, Table 2). The greater flexibility in the trophic modes of dinoflagellates compared with diatoms (Kudela et al., 2010; Smayda 2010; Jeong 2010; Flynn et al. 2013) can explain their

usually larger contribution to total phytoplankton C-biomass in the area of study (Table 2), where nutrients appear to be limiting. Some dinoflagellate genera (eg. *Heterocapsa*, *Gymnodinium*, *Scrippsiella*, *Procentrum*) are able to store nutrients under N or P limiting conditions (Smalley et al. 2003, Kudela et al., 2008; Flynn et al. 2013) and/or to switch to an heterotrophic mode under these conditions (Smalley et al., 2003). N deficiency during our samplings (N:P ratios <6) was registered during the MOUP and RELAX phases and this could have favoured a mixed dominance of autotrophic and/or mixotrophic dinoflagellates and diatoms. On the other hand, the nanoflagellates displayed very little seasonality in abundance with respect to the upwelling phases during the present study, this being consistent with results from other permanent (Herrera & Escribano, 2006; Rodriguez et al., 2006) and seasonal coastal upwelling areas (Casas et al., 1999; Tilstone et al., 2003; Barlow et al., 2005; Böttjer & Morales, 2007). In terms of C-biomass, however, this group did show a seasonality (higher in RELAX and WEKUP), suggesting that there are significant temporal changes in their size structure. Overall, the abundance and biomass of nanoflagellates (which does not include nanodino­flagellates) in the area of study was considerably lower to that reported in other coastal upwelling areas in the CCS System (Aristegui et al., 2004; Baltar et al., 2009) and other similar systems (Garrison et al., 1998; Böttjer & Morales, 2007; Crespo et al., 2012; Espinoza et al., 2012), although they made the most important contributions to Chl-a biomass; this difference is important in terms of C:Chl-a conversions usually applied for estimating C-biomass in the oceans.

The spatial variability in the abundance of the planktonic components was mostly attributable to differences between the most costal station E1 and the rest (Figs. 7 and 8), in particular during the MOUP and WEKUP phases (Figs. 11 and 12), in coincidence with the cross-shelf variability in the oceanographic conditions. The

functional group which primarily contributed to the dissimilarity were the FL (35%; greater WEKUP) and, secondarily, DIAT (25%) and DIN (23%). However, DIAT did contributed the most (35%) to the dissimilarity between the coastal (E2, E3, E4) and the coastal transition stations (E5, E6, E7), with secondary contributions from FL (29%) and DIN (24%). Differences in the composition of functional groups in the area off Cape Ghir were examined previously by Garcia et al. (2005), in comparing waters inside and outside the C. Ghir filament, with DIAT being more abundant inside and DIN outside the structure. During our samplings, a tongue of cold water was most evident during the MOUP phase and the sampling transect was fully included within it during Aug-09 but none of the geostrophic velocity fields, nor the Chl-a distribution, suggested that this structure represents a typical filament (Fig. 2).

Overall, our results indicate that the planktonic community off C. Ghir, including the coastal upwelling and the coastal transition zone, is usually represented (in terms of C-biomass) by a mixture of functional groups. In contrast, diatoms have been found to be dominant during the upwelling season in other eastern boundary current systems (Hutchings et al., 1995; Herrera & Escribano, 2006; Gonzalez et al. 2007; Kudela et al., 2008). Recently nanoflagellates have been described as the dominant components of the autotrophic biomass in the Iberian system, and mixotrophy as a dominant trophic function has been proposed for that system (Espinoza et al. 2012; Crespo et al. 2012). However, we suspect that these results are biased with regard to the methodological estimates of microplankton abundance (use of not representative counts per field) and biomass (suboptimal optical resolution for estimating cell volume in different taxa or functional groups and less accurate conversion factors for volume to carbon transformations). A mixture of functional groups in the area off Cape Ghir could be associated with the peculiar characteristics of its coastal upwelling, where relatively weak to moderate winds are dominant, contributing to

low to moderate levels of turbulence, and where the nutrient content of the upwelled waters is relatively low and where the highest values are restricted to the most inshore area. These environmental conditions will be more favourable to the presence and persistence of smaller size fractions in the phytoplankton and/or the dominance of flagellates and dinoflagellates in the coastal and the adjacent coastal transition zones, together with diatoms and autotrophic ciliates. Also, a mixotrophic strategy is expected to be favourable under such a system.

4.3. Plankton heterotrophic:autotrophic ratios in the upwelling system off Cape Ghir: implications for ecosystem functioning

During this study, the average H:A biomass ratios in the area off Cape Ghir were estimated to be >1 during the 3 samplings in which pico- to microplanktonic communities were sampled (Table 7). According to Gasol et al. (1997), these values are representative of relatively straight to inverse pyramids and not of a normal pyramid ($H:A < 1$) as it is expected for productive systems, such as coastal upwelling areas. One of the critical aspects in the calculation of H:A ratios is the inclusion/exclusion of mixotrophy ($H_m:A_m$, Gasol et al., 1997). This aspect is most critical for the microplankton size fraction as most of the techniques traditionally used in the identification and counting of the components do not include an estimation of their autofluorescence and, therefore, the trophic mode cannot be determined but only by literature. In applying a correction for mixotrophy in the estimation of the autotrophic biomass to our database, we obtained a $\sim 100\%$ decrease in the H:A ratios described above (Table 7); this suggests that a normal pyramid was representative of the WEKUP phase and a straight pyramid in the MOUP phase. The lack of a normal pyramid during the latter can be explained by factors such as nutrient limitation or an increase in the concentration of detritus in the water column (Cho and Azam, 1990;

Roman et al., 1995; Gasol et al., 1997).

A second critical aspect in the calculation of H:A biomass ratios relates to the diverse methodologies with which estimations of cellular volume and carbon content are made for planktonic components (Menden-Deuer & Lessard, 2000). In terms of biovolume estimations, these are based on the linear dimensions that can be measured and, based on the shape, they are transformed to volume (Eppley et al. 1970; Heinbokel 1978; Putt & Stoecker 1989; Borsheim & Bratbak 1987; Lessard 1991; Montagnes et al 1994; Menden-Deuer & Lessard, 2000). This calculation can be biased if the cell shape is more complex than the standard geometric forms used in the calculations (Chrzanowski & Simek, 1990; Sun & Liu 2003) or/and by the distortion of the volume that can be caused by the fixative used (Choi & Stoecker, 1989). In our case, we do not expect a large bias due to this aspect since we used volume estimates which have been previously standardized for pico- to microplanktonic components in the region of study (Ojeda, 1998; Zubkov et al., 1998, 2000; Fukuda et al., 1998), and most of the different components were identified and measured in great detail as to accurately estimate their carbon content (Table 3). Additionally, variability in cell size of the different plankton species or functional groups is common (Tomas et al., 1997) and this variability would strongly affect the use of average C-estimates (see examples in Table 3). In our case, for example, we applied an intermediate value for the C-biomass of autotrophic PEU but the size can vary between $1.15 \mu\text{m}^3$ and $2.45 \mu\text{m}^3$ (Calvo-Díaz et al., 2008); therefore, their contribution, which was important (Table 7), could have been 10 times lower or higher than that value if we had included size variation during the samplings.

In estimating the H:A biomass ratios, Gasol et al. (1997) included a wide range of sizes (pico- to mesoplankton) whereas existing estimates for the CCS have only included the pico- and nanoplankton fractions (including flagellates and

dinoflagellates together) and the ratios in the latter ranged between 0.9 and 4.1 (Arístegui et al., 2004., 2005; Baltar et al., 2009). In calculating our H:A ratios with these two fractions only (pico-and nanoflagellates, including NFL and NDIN), the values decreased slightly (0.6-0.8). However, the contribution of the microplankton fraction to C-biomass is important in the coastal area off C. Ghir and cannot be ignored in the H:A calculation.

Conclusions

Cape Ghir is characterized as an area of permanent upwelling and here we have shown that both, spatial and temporal changes in the upwelling conditions are strongly associated with variations in the planktonic community structure. This community is represented mostly by mixed assemblages of, mainly, dinoflagellates, ciliates, and diatoms and C-biomass is dominated by the microplankton fraction. A detailed analysis of the taxa represented in these functional groups, allowed us to made very fine estimates of C-biomass and, at the same time, to evaluate the contribution of specific taxa to mixotrophy. This analysis resulted to be very revealing with regard to the assessments of the heterotrophic:autotrophic biomass ratios in marine systems; when the contribution of mixotrophs was considered, the mean values were <1 (normal pyramid) but changed to >1 without it. On the other hand, total Chl-a was mainly dominated by nanoplankton fraction whereas diatoms and dinoflagellates in the microplankton fraction were the main contributors to the the autotrophic (including a portion of the mixotrophs) biomass during this study. This implies that simple C:Chl-a conversions usually used are not appropriate for this area. This is probably related to a suboptimal physiological state in the case of the diatoms (nutrient limitation, particularly Si and N) and/or a significant contribution of

mixotrophic and microplanktonic dinoflagellates and ciliates. Undoubtedly, these matters require further research, and over longer time series, before understanding the factors that modulate the observed responses of the plankton to variability in the upwelling conditions in the area of study.

Acknowledgements.

Esta investigación se llevó a cabo en el marco del proyecto IMBER, aprobado CAIBEX (CTM2007-66408-CO2-02) "Plan Nacional español de I + D" (MEC), coordinado por Dr. J.A. Quiero dar mis más sentidos agradecimientos a la Dra. Carmen Morales, por su inagotables aportes, por animarme, apoyarme en los ratos mas difíciles, por permitirme seguir desarrollándome y por sobre todo por su paciencia y generosidad. Al Dr. Javier Aristegui, por su tiempo y apoyo. A mis compañeras Minerva Espino, Mar Benavides, por apoyarme en los analizar de nutrientes y preparación de material de embarque. A la Dra. María Fernanda Montero y Dr. Javier Aristegui, por realizar los análisis de citometría. Al Dr. Samuel Hormazábal por facilitar su equipo de trabajo, Marco Corea e Isabel Andrade para generar las imágenes Satelital de Temperatura, Viento y Clorofila. A los Drs. O. Ettahiri, A. Makaoui y A. Orbi por su apoyo en terreno y facilitar los datos hidrográficos. Finalmente quiero agradecer a todos los miembros del laboratorio B-201, especialmente a Cory por ayudarme en la digitación de algunos análisis biológicos y a mis amigos Raul Santana y Federico Maldonado por su inestimable amistad. Además agradezco a los capitanes y tripulaciones de los "Amir Moulay Abdellah (AMA)" R / Vs y "Sarmiento de Gamboa", así como el personal técnico, por su inestimable ayuda en el mar. A CONICYT que financio mis estudios de postgrado en la ULPGC. y al Proyecto CONICYT-FONDECYT 1120504. Esta memoria constituye un manuscrito que está siendo sometido al Progress in Oceanography.

Y siempre gracias a mis padres y hermana, por apoyarme a seguir en esta loca aventura

References

- Adolf JE., Stoecker, D.K., Harding, L.W., 2006 The balance of autotrophy and heterotrophy during mixotrophic growth of *Karlodinium micrum* (Dinophyceae). *Journal Plankton Research*. 28, 737- 751.
- Anderson, O. R., Nigrini, N., Boltovskoy, D., Takahashi, K., Swanberg, N., 2002. Class Polycystinea. En: Lee, J. (ed.). *An Illustrated Guide to the Protozoa*, 2nd Protozoologists, Lawrence, Kansas, pp. 371-656.
- Arístegui, J. and Harrison, W.G., 2002. Decoupling of primary production and community respiration in the ocean: implications for regional carbon studies. *Aquatic Microbial Ecology*, 29, 199-209.
- Arístegui, J., Barton, E.D., Tett, P., Montero, M.F., García-Muñoz, M., Basterretxea, G., Cussatlegras, A.S., Ojeda, A., de Armas, D., 2004. Variability in plankton community structure, metabolism, and vertical carbon fluxes along an upwelling filament (Cape Juby, NW Africa). *Progress in Oceanography*. 62, 95–113.
- Arístegui, J. and Montero, M.F., 2005. Temporal and spatial changes in microplankton respiration and biomass in the Canary Islands: the effect of mesoscale variability. *Journal of Marine Systems*. 4, 65-82
- Arístegui, J., Álvarez-Salgado, X.A., Barton, E.D., Figueiras, F.G., Hernández-León, S., Roy, C., Santos, A.M.P., 2006. Oceanography and fisheries of the Canary Current Iberian region of the Eastern North Atlantic. In: Robinson, A., Brink, K.H. (Eds.), *The Global Coastal Ocean: Interdisciplinary Regional Studies and Syntheses, The Sea: Ideas and Observations on Progress in the Study of the Seas*,

- vol. 14. Harvard University Press, pp. 877–931.
- Arístegui J., Barton E.D., Álvarez-Salgado, X.A., Santos A.M.P., Figueiras, F.G., Kifani, S., Hernández-León, S., van Mason, E., Machú, E., Demarcq, H., 2009. Sub-regional ecosystem variability in the Canary Current upwelling. *Progress in Oceanography*. 83, 33-48.
- Baltar, F., Arístegui, J., Montero, M.F., Espino, M., Gasol, J.M., Herndl, G.J., 2009. Mesoscale variability modulates seasonal changes in the trophic structure of nano- and picoplankton communities across the NW Africa–Canary Islands transition zone. *Progress in Oceanography*. 83 (1–4), 180–188.
- Barlow, R., Sessions, H., Balarin, M., Weeks, S., Whittle, C., Hutchings, L., 2005. Seasonal variation in phytoplankton in the southern Benguela: pigment indices and ocean colour. *South African Journal of Marine Science*. 27 (1), 275–287.
- Barton, E.D., Arístegui, J., Tett, P., Cantón, M., García-Braun, J., Hernández-León, S., Nykjaer, L., Almeida, C., Almunia, J., Ballesteros, S., Basterretxea, G., Escánez, J., García-Weill, L., Hernández-Guerra, A., López-Laatzén, F., Molina, R., Montero, M.F., Navarro-Pérez, E., Rodríguez, J.M., van Lenning, K., Vélez, H. and Wild, K. 1998. The transition zone of the Canary Current upwelling region. *Progress in Oceanography*. 41, 455-504.
- Bernard, C., and Rassoulzadegan, F. 1994. Seasonal variations of mixotrophic ciliates in the northwestern Mediterranean Sea. *Marine Ecology Progress Series*. 108, 295-301.
- Böttjer, D., and Morales, C.E., 2007. Nanoplanktonic assemblages in the upwelling area off Concepción (36°S), central Chile: abundance, biomass, and grazing potential during the annual cycle. *Progress in Oceanography*. 75, 415–434.
- Børsheim, K.Y. and Bratbak, G., 1987. Cell volume to cell carbon conversion factor for a bacterivorous *Monas* sp. enriched from seawater. *Marine Ecology Progress*

Series. 36, 171–175

- Bowden, K.F., 1983. *Physical Oceanography of Coastal Waters*. In: Ellis Horwood Series on Marine Science. John Wiley & Sons, New York, 302 pp.
- Burkholder J.A.M., Glibert P.M., Skelton H.M., 2008. Mixotrophy, a major mode of nutrition for harmful algal species in eutrophic waters. *Harmful Algae*. 8, 77-93.
- Calvo-Díaz, A., Morán, X.A.G., Suárez L.A., 2008 Seasonality of picophytoplankton chlorophyll a and biomass in the central Cantabrian Sea, southern Bay of Biscay. *Journal Marine Systems*. 72, 271–281.
- Casas, B., Varela, M., Bode, A., 1999. Seasonal succession of phytoplankton species on the coast of A Coruña (Galicia, northwest Spain). *Boletín Instituto Español Oceanografía*. 15 (1–4), 413–429.
- Chavez, F.P. and Messié, M., 2009. A comparison of eastern boundary upwelling systems. *Progress in Oceanography*. 83 (1–4), 80–96.
- Cho, B. C., and Azam, F., 1990. Biogeochemical significance of bacterial biomass in the ocean's euphotic zone. *Marine Ecology Progress Series*. 63, 253–259.
- Choi, J.W. and Stoecker, D.K., 1989. Effects of fixation on cell volume of marine planktonic protozoa. *Applied and Environmental Microbiology*. 55 (7), 1761–1765.
- Chrzanowski, T.H. and Simek, K., 1990. Prey-size selection by freshwater flagellated protozoa. *Limnology and Oceanography*. 35 (7), 1429–1436.
- Clarke KR, Warwick RM (2001) *Change in marine communities: an approach to statistical analysis and interpretation*, Primer-e, Plymouth
- Clarke, K.R., Gorley, R.N., 2006. *PRIMER v6: User Manual/Tutorial*. PRIMER-E: Plymouth.

- Crespo, B.G., Espinoza-González, I.O., Teixeira, I.G., Castro, C.G., Figueiras, F.G., 2012. Structure of the microbial plankton community in the NW Iberian margin at the end of the upwelling season. *Journal of Marine Systems* 95, 50–60.
- Espinoza-González, I.O., Figueiras, F.G., Crespo, B.G., Teixeira, I.G., Castro, C.G., 2012. Autotrophic and heterotrophic microbial plankton biomass in the NW Iberian upwelling: seasonal assessment of metabolic balance. *Aquatic Microbial Ecology*. 67, 77–89.
- Eppley, R. W., Reid, F. M. H., Strickland, J. D. H. (1970). The ecology of plankton off La Jolla, California, in the period April to September 1967. Estimates of phytoplankton crop size, growth rate and primary production. *Bulletin Scripps Institution of Oceanography*. 17: 33-4.
- Fanning, K.A., 1992. Nutrient Provinces in the Sea: Concentration Ratios, Reaction Rate Ratios, and Ideal Covariation. *Journal of Geophysical Research*. 97 (C4), pages 5693 – 5712.
- Flynn, K.J., Stoecker D.K., Mitra A., Raven, J.A., GLIBERT, P.M., Hansen, P.J., Granèli, D. and Burkholder, J.M., 2013. Misuse of the phytoplankton– zooplankton dichotomy: the need to assign organisms as mixotrophs within plankton functional types. *J. Plankton Res.* (2013) 35(1): 3–11.
- Fréon, P., Arístegui, J., Bertrand, A., Crawford, R.J.M., Field, J.C., Gibbons, M.J., Tam, J., Hutchings, L., Masski, H., Mullon, C., Ramdani, M., Seret, B., Simier, M., 2009. Functional group biodiversity in eastern boundary upwelling ecosystems questions the wasp-waist trophic structure. *Progress in Oceanography*. 83 (1– 4), 1–14.
- Freudenthal, T., Neuer, S., Meggers, H., Davenport, R., Wefer, G., 2001a. Influence of lateral particle advection and organic matter degradation on sediment accumulation and stable nitrogen isotope ratios along a productivity gradient in the

- Canary Islands region. *Marine Geology*. 177 (1–2), 93–109.
- Freudenthal, T., Meggers, H., Henderiks, J., Kuhlmann, H., Moreno, A., and Wefer, G., 2002. Upwelling intensity and filament activity off Morocco during the last 250,000 years, *Deep-Sea Research I*. 49 (17), 3655-3674.
- Fukuda, R., Ogawa, H., Nagata, T., Koike, I., 1998. Direct determination of carbon and nitrogen content of natural bacteria assemblages in marine environments. *Applied Environmental Microbiology*. 64, 3352–3358.
- García-Muñoz, M., Arístegui, J., Pelegrí, J.L., Antoranz, A., Ojeda, A., Torres, M., 2005. Exchange of carbon by an upwelling filament off Cape Guir (NW Africa). *Journal of Marine Systems*, 54, 83-95.
- Garrison, D.L., Gowing, M.M., Hughes, M.P., 1998. Nano- and microplankton in the northern Arabian Sea during the Southwest Monsoon. August–September 1995. A US-JGOFS study. *Deep-Sea Research. II* 45, 2269–2299.
- Gasol, J.M., del Giorgio, P.A., Duarte, C.M., 1997. Biomass distribution in marine planktonic communities. *Limnology and Oceanography*. 42, 1353-1363.
- González, H.E., Menschel, E., Aparicio, C., Barría, C., 2007. Spatial and temporal variability of microplankton and detritus, and their export to the shelf sediments in the upwelling area off Concepción, Chile (36°S), during 2002–2005. *Progress in Oceanography*. 75, 435–451.
- Hagen, E., Zulicke, C., Feistel, R., 1996. Near-surface structures in the Cape Ghir filament off Morocco. *Oceanologica Acta*. 19, 577-598
- Hasle, G.R. and Syvertsen, E., 1997. Marine Diatoms. In: Tomas, C.R. (Ed.), *Identifying marine phytoplankton*. Academic Press, San Diego/ London. pp. 5–386.
- Head, E.J.H., Harrison, W.G., Irwin, B.I., Horne, E.P.W., Li, W.K.W., 1996. Plankton dynamics and carbon flux in an area of upwelling off the coast of Morocco. *Deep-*

- Sea Research I. 43, 1713-1738.
- Heinbokel, J.F., 1978. Studies on the functional role of tintinnids in the southern California Bight. I. and II. *Marine Biology*. 47, 177–197
- Hernández-Guerra, A. and Nykjaer, L., 1997. Sea surface temperature variability off north-west Africa: 1981–1989. *International Journal of Remote Sensing*. 18, 2539–2558.
- Herrera, L. and Escribano, R., 2006. Factors structuring the phytoplankton community in the upwelling site off El Loa River in northern Chile. *Journal Marine Systems*. 61, 13–38.
- Holm-Hansen, O., Lorenzen, C.J., Holmes, R.W., Strickland, J.D.H., 1965. Fluorometric determination of chlorophyll. *J. Conseil Int. pour l'Exploration de la Mer*. 30, 3–15.
- Hood, R.R., Neuer, S., Cowles, T., 1992. Autotrophic production, biomass, and species composition at two stations across an upwelling front. *Marine Ecology Progress Series*. 83, 221–232.
- Hutchings, L., Pitcher, G.C., Probyn, T.A., Bailey, G.W., 1995. The chemical and biological consequences of coastal upwelling. In: summerhayes, C.P., Emeis, K.-C., Angel, M.V., Smith, R.L., Zeitzschel, B. (Eds.), *Upwelling in the Ocean Modern Processes and ancient records*. Dahlem Workshop Reports. Environmental Sciences Research Report 18. Wiley Publishers, pp. 67–72.
- Hutchings, L., van der Lingen, C., Shannon, L., Crawford, R., Verheye, H.M.S., Bartholomae, C., van der Plas, A., Louw, D., Kreiner, A., Ostrowski, M., Fidel, Q., Barlow, R., Lamont, T., Coetzee, J., Shillington, F., Veitch, J., Currie, J., Monteiro, P., 2009. The Benguela current: an ecosystem with four components. *Progress in Oceanography*. 83 (1–4), 15–32.
- Jacobson, D.M. and Andersen, R.A., 1994. The discovery of mixotrophy in

photosynthetic species of *Dinophysis* (Dinophyceae): light and electron microscopical observations of food vacuoles in *Dinophysis acuminata*, *D. norvegica* and two heterotrophic dinophysoid dinoflagellates. *Phycologia*. 33, 97-110

Jeong HJ, Yoo YD, Kang NS, Rho JR, Seong KA, Park JW, Nam GS, Yih WH (2010) Ecology of *Gymnodinium aureolum*. I. Feeding in western Korean water. *Aquatic Microbial Ecology*. 59, 239-25.

Kang, N.S., Jeong, H.J., Moestrup, Ø., Shin, W.G., Nam, S.W., Park, J.Y, de Salas, M.F, Kim, K.W., Noh, J.H., 2010. Description of a new planktonic mixotrophic dinoflagellate *Paragymnodinium shiwhaense* n. gen., n. sp. from the coastal waters off western Korea: morphology, pigments, and ribosomal DNA gene sequence. *Journal Eukaryotic Microbiology*. 57, 121-144

Keister, J.E., Peterson, W.T., Pierce, S.D., 2009a. Zooplankton distribution and cross-shelf transfer of carbon in an area of complex mesoscale circulation in the northern California Current. *Deep Sea Research I*. 56, 212-231.

Kudela, R., Pitcher, G., Probyn, T., Figueiras, F., Moita, T., Trainer, V., 2005.

Harmful

algal blooms in coastal upwelling system *Oceanography*. 18, 184–197.

Kudela, R., Ryan, J., Blakely, M., Lane, J., Peterson, T., 2008. Linking the physiology and ecology of *Cochlodinium* to better understand harmful algal bloom events: a comparative approach. *Harmful Algae*. 7, 278–292.

Kudela, R.M., Seeyave, S., Cochlan, W.P., 2010. The role of nutrients in regulation and promotion of harmful algal blooms in upwelling systems. *Progress in Oceanography*. 55, 122–135

Lachkar, Z. and N. Gruber, N., 2012. A comparative study of biological production in eastern boundary upwelling systems using an artificial neural network.

- Biogeosciences. 9, 293–308.
- Largier, J.L., Magnekl, B.A., Winant, C.D., 1993. Subtidal circulation over the Northern California shelf. *Journal of Geophysical Research*. 98, 18147-181179.
- Lauthuilière, C., Echevin, V., Lévy, M., 2008. Seasonal and intraseasonal surface chlorophyll-a variability along the northwest African coast. *Journal of Geophysical Research*. 113, C05007, doi:10.1029/2007JC004433
- Lessard, E. J. 1991. The trophic role of heterotrophic dinoflagellates in diverse marine environments. *Marine Microbial Food Webs*. 5, 49-58.
- Lynn, D. H. and Small, E. B., 2002. Phylum Ciliophora. En: Lee, J. J., Bradbury, P. C., Leedale, G. F. (eds.). *An Illustrated Guide to the Protozoa*. Society of edn. Society of Protozoologists, Lawrence, KS. pp. 994-1022.
- Mackas, D., Strub, P.T., Thomas, A.C., Montecino, V., 2006. Eastern ocean boundaries pan-regional view. In: Robinson, A.R., Brink, K.H. (Eds.). *The Sea*. Harvard Press Ltd., Boston. Chapter 2, pp. 21-60.
- Marcello, J., Hernandez-Guerra, A., Eugenio, F. and Fonte, A., 2011. Seasonal and temporal study of the northwest African upwelling system. *International Journal of Remote Sensing*. 32 (7), 1843–1859
- Margalef, R., 1978. Life-forms of phytoplankton as survival alternatives in an unstable environment. *Oceanologica Acta*. 1, 493–509.
- Menden-Deuer, S. and Lessard, E.J., 2000. Carbon to volume relationships for dinoflagellates, diatoms, and other protist plankton. *Limnology and Oceanography*. 45 (3), 569–579.
- Montagnes, D.J., Berges, J.A., Harrison P.J., and Taylor F.J., 1994. Estimating carbon, nitrogen, protein and chlorophyll a from volumen in marine phytoplankton. *Limnology and Oceanography*. 39: 1044-1060
- Morales, C.E. and Anabalón, V., 2012. Phytoplankton biomass and microbial

- abundances during the spring upwelling season in the coastal area off Concepción, central-southern Chile: Variability around a time series station. *Progress in Oceanography*. 83 (1–4), 80–96.
- Neuer, S., Freudenthal, T., Davenport, R., Llinás, O., Rueda, M.J., 2002. Seasonality of surface water properties and particle flux along productivity gradient off NW Africa. *Deep Sea Research II*. 49, 3561-3567
- Nieto, N., Demarcq, H., McClatchie, S., 2012. Mesoscale frontal structures in the Canary Upwelling System: New front and filament detection algorithms applied to spatial and temporal patterns. *Remote Sensing of Environment*. 123, 339–346
- Nykjaer, L. and Van Camp, L., 1994. Seasonal and interannual variability of coastal upwelling along Northwest Africa and Portugal from 1981 to 1991. *Journal of Geophysical Research*. 99 (C7), 14197-14207.
- Ojeda, R. A., 1998. *Dinoflagelados de Canarias: estudio taxonómico y ecológico*, Universidad de Las Palmas de Gran Canaria. ULPGC, Las Palmas de Gran Canaria. 438 pp.
- Pelegrí, J.L., Aristegui, J., Cana, L., González-Dávila, M., Hernández-Guerra, A., Hernández-León, S., Marrero-Díaz, A., Montero, M.F., Sangrá, P., Santana-Casiano, M., 2005a. Coupling between the open ocean and the coastal upwelling region off northwest Africa: water recirculation and offshore pumping of organic matter. *Journal of Marine Systems*. 54, 3-37.
- Pelegrí, J.L., Marreno-díaz, A., Ratsimandresy, A., Antoranz, A., Cisneros-Aguirre, J., Gordo, C., Grisolia, D., Hernández-guerra, A., Láiz, I., Martínez, A., Parrilla, G., Pérez-Rodríguez, P., Rodríguez-Santana, A., Sangrá, P., 2005b. Hydrographic cruises off northwest Africa: the Canary Current and the Cape Ghir region. *Journal of Marine Systems*. 54, 39-63.
- Probyn, T.A., 1992. The inorganic nutrition of phytoplankton in the southern

- Benguela: new production, phytoplankton size and implications for pelagic food webs. *South African Journal of Marine Science*. 12, 411–420.
- Putt, M. and Stoecker, D.K., 1989. An experimental determined carbon: volume ratio for marine "oligotrichous" ciliates from estuarine and coastal waters. *Limnology and Oceanography*. 34, 1097-1103.
- Rodríguez, F., Garrido, J.L., Crespo, B.G., Arbones, B., Figueiras, F.G., 2006. Size-fractionated phytoplankton pigment groups in the NW Iberian upwelling system: impact of the Iberian Poleward Current. *Marine Ecology Progress Serie*. 323, 59–73.
- Roman, M.R., Caron, D.A., Kremer, P., Lessard, E.J., Madin, L.P., Malone, T.C., Napp, J.M., Peele E.R., Youngblutii, M. J., 1995. Spatial and temporal changes in the partitioning of organic carbon in the plankton community of the Sargasso Sea off Bermuda. *Deep-Sea Research*. 42, 973-992.
- Romero, O.E., Lange, C.B., and Wefer, G., 2002. Interannual variability (1988-1991) siliceous phytoplankton fluxes off northwest Africa. *Journal of Plankton Research*. 24 (10), 1035-1046.
- Shannon, L.V., Walters, N.M., Mostert, S.A., 1985. Satellite observations of surface temperature and near-surface chlorophyll in the southern Benguela region. In: Shannon, L.V. (Ed.), *South African Ocean Colour and Upwelling Experiment*. Sea Fisheries Research Institute. Cape Town, pp. 183-210.
- Sherr, E.B., Sherr, B.F., Longnecker, K., 2006. Distribution of bacterial abundance and cell-specific nucleic acid content in the Northeast Pacific Ocean. *Deep-Sea Research I*. 53, 713–725.
- Sicre, M.A., Ternois Y., Paterne, M., Martinez P., Bertrand P., 2001. Climatic changes in the upwelling region off Cap Blanc NW Africa over the last 70 k year: a multi-biomarker approach. *Org Geochem*, 32:981–990.

- Smalley, G.W., Coats, D.W., Stoecker, D.K., 2003. Feeding in the mixotrophic dinoflagellate *Ceratium furca* is influenced by intracellular nutrient concentrations. *Marine Ecology Progress Series*. 262, 137–151.
- Smayda, T.J., 2010. Adaptations and selection of harmful and other dinoflagellate species in upwelling systems 1. Morphology and adaptive polymorphism. *Progress in Oceanography*. 85, 53–70.
- Stoecker, D. K., Michaels, A. E., Davis, L. H. (1987). A large fraction of marine planktonic ciliates can contain functional chloroplasts. *Nature*. 326, 790-792.
- Stoecker, D. K., Taniguchi, A., Michaels, A. E. (1989). Abundance of autotrophic, mixotrophic and heterotrophic planktonic ciliates in shelf and slope waters. *Marine Ecology Progress Series*. 50, 241-254.
- Stoecker, D.K., Gustafson, D. E. & Verity, P. G., 1996. Micro- and mesoprotozooplankton at 140° W in the equatorial Pacific: Heterotrophs and mixotrophs. *Aquatic Microbiology Ecology*. 10, 273-282.
- Sun, J., and Lui, D., 2003. Geometric models for calculating cell biovolume and surface area for phytoplankton. *Journal Plankton Research*. 25 (11), 1331–1346.
- Tilstone, G.H., Figueiras, F.G., Lorenzo, L.M., Arbones, B., 2003. Phytoplankton composition, photosynthesis and primary production during different hydrographic conditions at the Northwest Iberian upwelling system. *Marine Ecology Progress Series*. 252, 89–104.
- Thiel, M., Macaya, E.C., Acuña, E., Arntz, W.E., Bastias, H., Brokordt, K., Camus, P. A., Castilla, J.C., Castro, L.R., Cortes, M., Dumont, C.P., Escribano, R., Fernandez, M., Gajardo, J.A., Gaymer, C.F., Gomez, I., Gonzalez, A.E., Gonzalez H.E., Haye P.A., Illanes J.E., Iriarte J.L., Lancellotti, D.A., Jorquera, G.L., Luxoro, C., Manriquez, P.H., Marin, V., Muñoz, P., Navarrete, S.A., Perez E., Poulin, E., Sellanes J., Sepulveda, H.H., Wolfgang, S., Tala F., Thomas, A., Vargas, C.,

- Vasquez, J.A., Alonso-Vega, J.M. 2007. The Humboldt current system of Northern and central Chile. *Oceanography and Marine Biology: An Annual Review*. **45**, 195-344.
- Thompson, G. A.. 2004. Tintinnid diversity trends in the southwestern Atlantic Ocean (29 to 60° S). *Aquatic Microbial Ecology*. **35**, 93-130.
- Treguer, P. and Le Corre, P., 1978. The ratios of nitrate phosphate, and silicate during uptake and regeneration phases of the Moroccan upwelling regime. *Deep-Sea Research*, Vol 26A, pp. 163-184.
- Tomas, C., 1997. *Identifying Marine Phytoplankton*. Academic Press. 858 pp
- UNESCO. (1994). *Protocols for the Joint Global Ocean Flux Study (JGOFS) Core Measurement*. Intergovernmental Oceanographic Commission. Manual and Guides 29, pp. 169.
- Van Camp, L., Nykjaer, L., Mittelstaedt, E., Schlittenhake, P., 1991. Upwelling and boundary circulation off Northwest Africa as depicted by infrared and visible satellite observations, *Progress in Oceanography*. **26**, 357-402.
- Verity, P. and Sieracki, M., 1993. Use of color image analysis and epifluorescence microscopy to measure plankton biomass: En: Kemp, P., Sherr, E. & Cole, J. (eds.): *Handbook of methods in aquatic microbial ecology*. Lewis Publisher, Boca Raton. 327-338.
- Villafañe, V. and Reid, F., 1995. *Metodos de microscopia para la cuantificación del fitoplancton*. In: Alveal, K., Ferrario, M.E., Oliveira, E.C., Sar, E. (Eds.), *Manual de métodos ecológicos*. Editorial Anibal Pinto, Universidad de Concepcion, Chile. pp. 169-185.
- Voituriez, B., Dufour, P. and Le Borgne, R., 1974. Preliminary results on R.V. *Capricorne* 74 02 cruise in CapeBlanc. *C.U.E.A. Newsletter*. **3(5)**, 1 - 7.
- Zar, J.H., 1984. *Biostatistical analysis*. Prentice-Hall International, Inc, New Jersey,

718 pp.

Zhao M., Eglinton G., Haslett S.K., Jordan R.W., Sarnthein M., Zhang Z., 2000.

Marine and terrestrial biomarker records for the last 35,000 years at ODP site 658C off NW Africa. *Organic Geochemistry*. 31(9), pp. 919-930.

Zubkov, M.V., Sleigh, M., Tarran, G.A., Burkill, P.H., Leakey, R.J.G., 1998.

Picoplankton community structure on an Atlantic transect from 50N to 50S. *Deep Sea Research I*. 45, 1339–1355.

Zubkov, M.V., Sleigh, M.A., Burkill, P.H., 2000. Assaying picoplankton distribution

by flow cytometry of underway samples collected along a meridional transect across the Atlantic Ocean. *Aquatic Microbial Ecology*. 21, 13 – 20.

Figure legends

Figure 1. a) Region of study off Cape Ghir in NW Africa; bathymetry and location of the 7 sampling stations are shown; b) Daily mean wind stress (N m^{-2}) in the sampling region; c) Satellite Sea Surface Temperature (SST in $^{\circ}\text{C}$) and d) Chlorophyll a (Chl-a in mg m^{-3}) time series data (June 2008 to December 2009) for the sampling region ($30.5\text{-}31.5^{\circ}\text{N}$; $9.5\text{-}11.5^{\circ}\text{W}$). Vertical broken-lines indicate dates of the in situ samplings.

Figure 2. Satellite data for the region around Cape Ghir ($32.5\text{-}29.5^{\circ}\text{N}$; $9.0 - 12.5^{\circ}\text{W}$) during the in situ samplings: wind velocity (m s^{-1}) and direction (left panels), SST ($^{\circ}\text{C}$; central panels), and Chl-a (mg m^{-3} ; right panels). The data correspond to 5 days averages (3 d before and 2 d during each sampling). The geostrophic velocity field (cm s^{-1}) is also shown in the two latter.

Figure 3. Distribution of oceanographic variables during each of the cruises off Cape Ghir: temperature ($^{\circ}\text{C}$; left panels), salinity (central-left panels), and sigma-t (kg m^{-3} ; central-right panels), and T/S diagrams (right panels).

Figure 4. Groups of sampling stations resulting from Multidimensional scaling (MDS) and cluster analyses based on the environmental variables (see Table 2 for the nomenclature of the stations).

Figure 5. Distribution of Chl-a concentration (mg m^{-3}) during each of the cruises off Cape Ghir: total and size fractions (micro-, nano-, and picoplankton, from left to right, respectively). Notice the different scale in the case of the picoplankton fraction.

Figure 6. Distribution of nanoplankton abundance (cells mL⁻¹) off Cape Ghir. Panels from left to right, respectively: NFL, NDIN, NDIAT, NCIL (see abbreviations in Table 4). Notice the change of scale for different groups.

Figure 7. Distribution of microplankton abundance (cells mL⁻¹) off Cape Ghir: MFL, MDIN, MDIAT, MCIL (see abbreviations in Table 4; panels from left to right, respectively). Notice the change of scale for different groups.

Figure 8. Relative contribution of planktonic groups off Cape Ghir in terms of integrated abundance (left panels) and biomass (right panels): a) total nano- and microplankton, b) total microplankton, and c) total nanoplankton.

Figure 9. Distribution of picoplankton abundance (cells mL⁻¹) off Cape Ghir (only 3 sampling dates): HB, SYN, PRO and PEUK (see abbreviations in Table 2; panels from left to right, respectively). Notice the change of scale for different groups.

Figure 10. Groups of sampling stations resulting from MDS and cluster analyses based on the biological variables related to the nano- and microplankton size fractions: a) integrated abundance, and b) integrated biomass (see Table 2 for the nomenclature of the stations).

Figure 11. Results of the LINKTREE analysis on the environmental variables that best explain the separation of the biological groups detected in Fig.10 along an axis of Bray-Curtis similarity (B%) for: a) integrated abundance, and b) integrated biomass in the nano- and microplankton size fractions.

Figure 12: Distribution of integrated (0-25 m depth) nutrients in the area off C. Ghir. Nitrate and nitrite ($\text{NO}_3 + \text{NO}_2$), phosphate (PO_4), and silicate (Si O_2), all in mmol m^{-2} , at each of the sampling stations and during the different samplings.

Figure 1

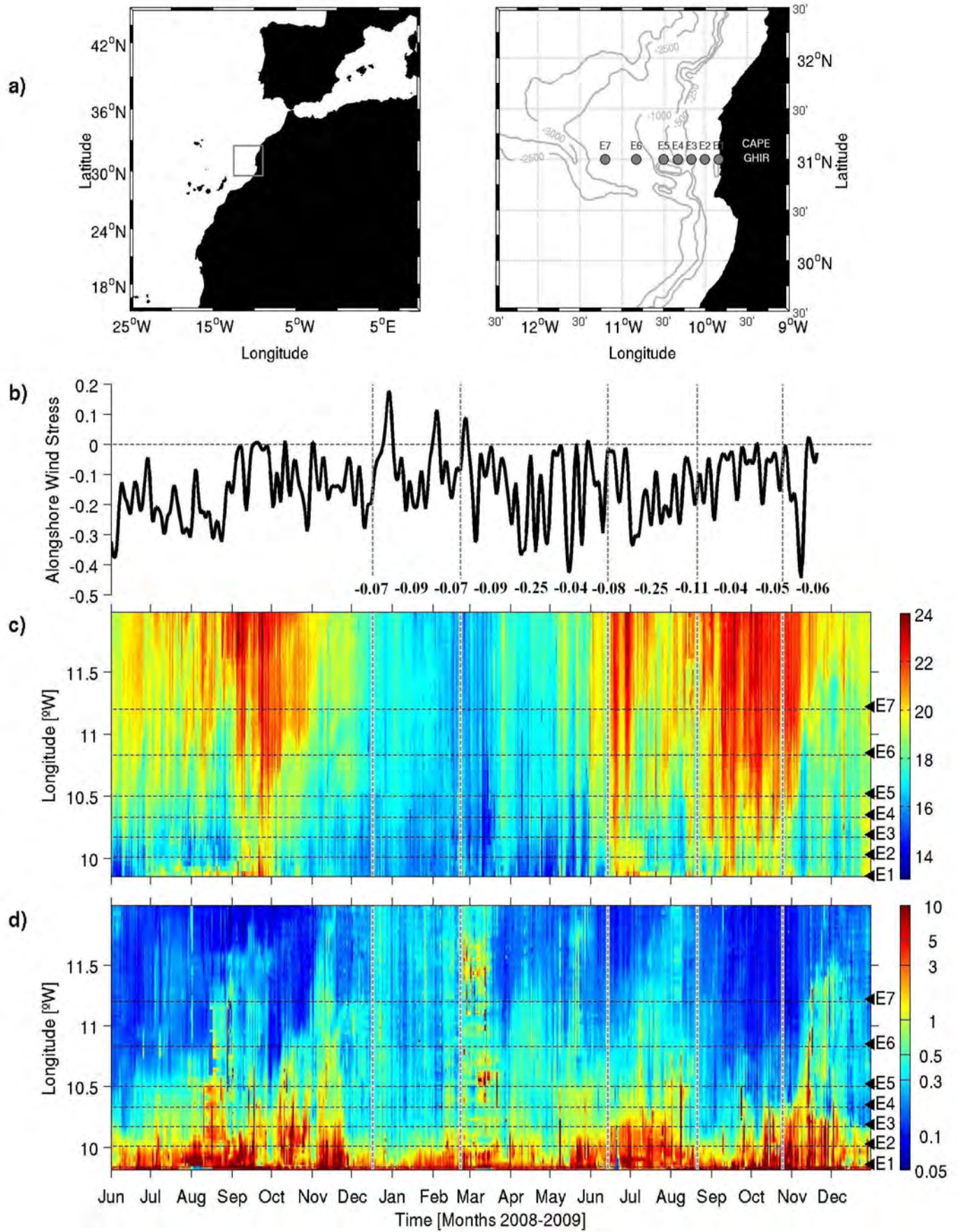


Figure 2

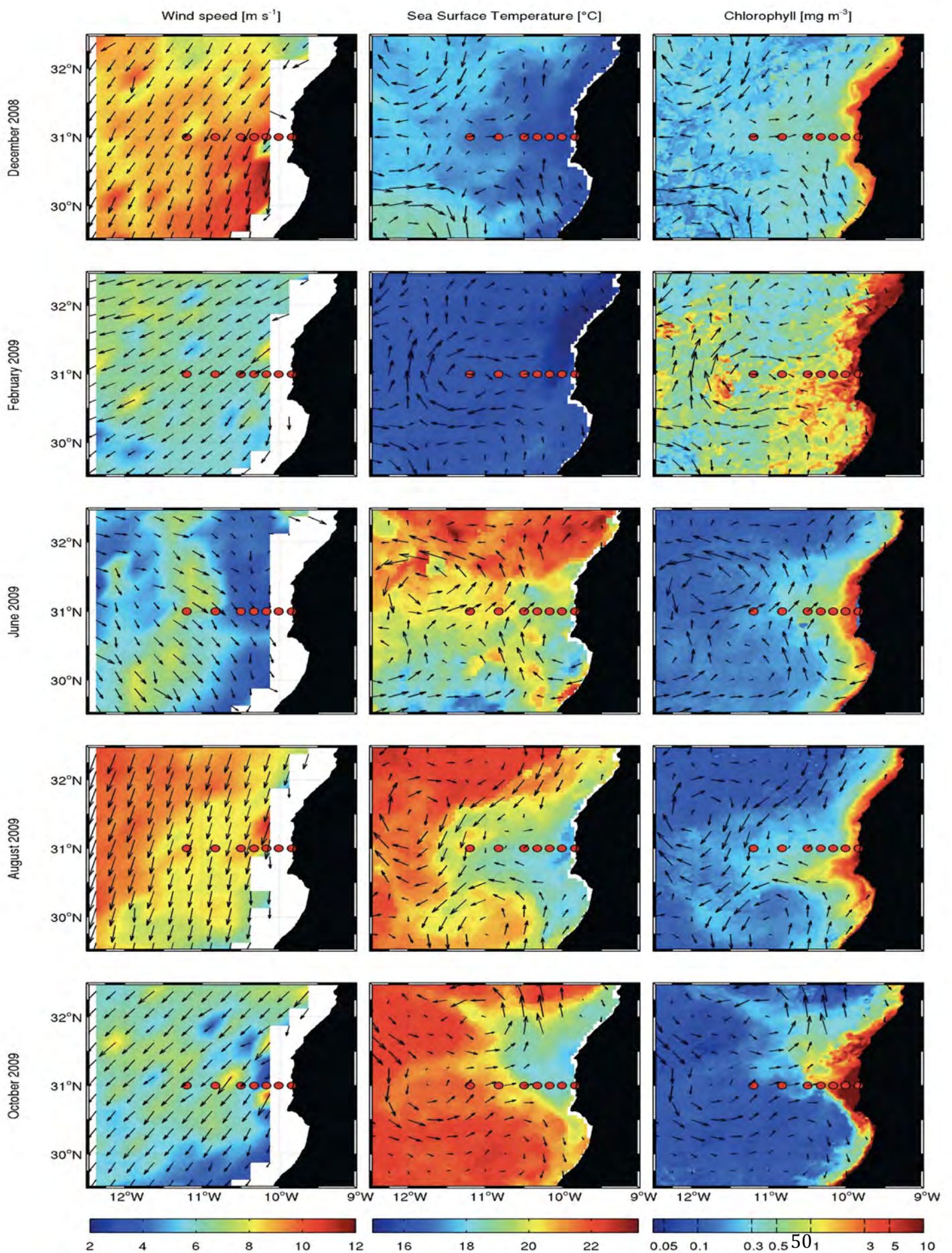


Figura 4

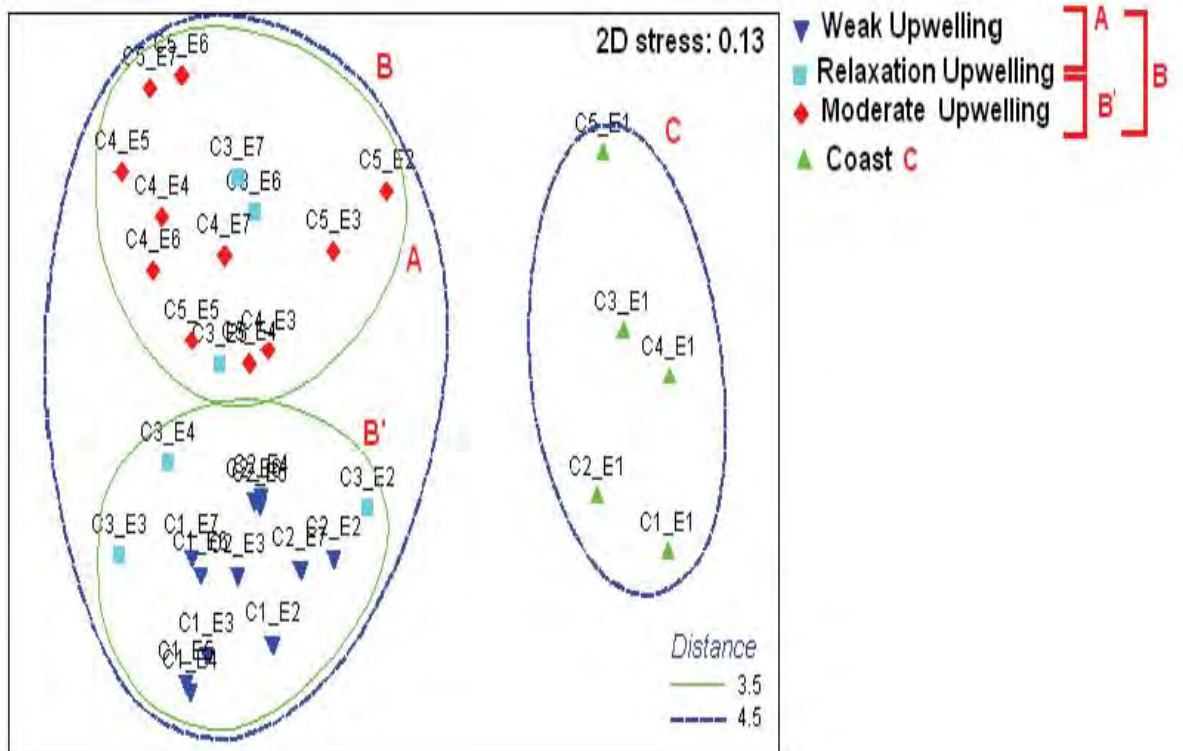


Figure 5

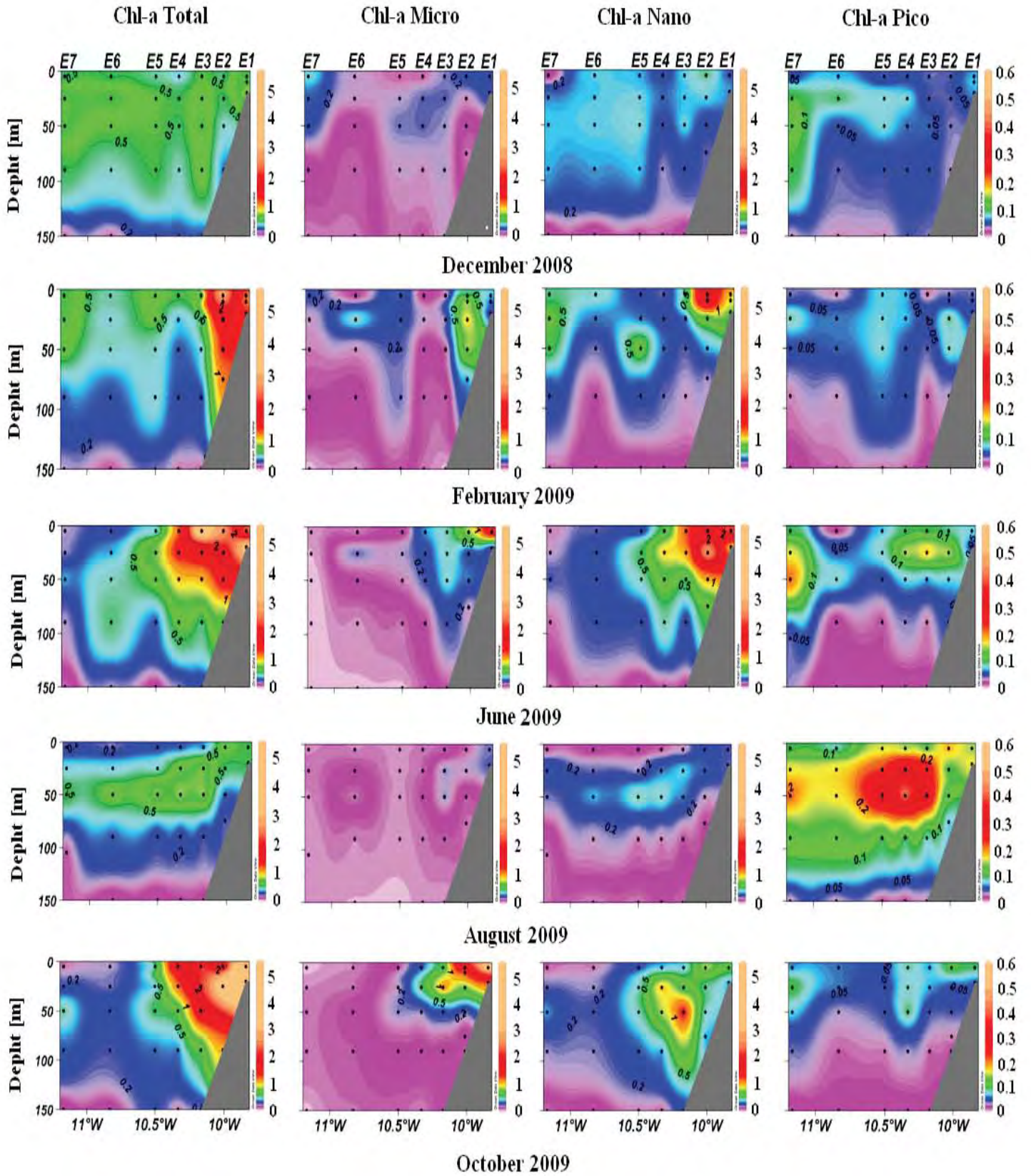


Figure 6

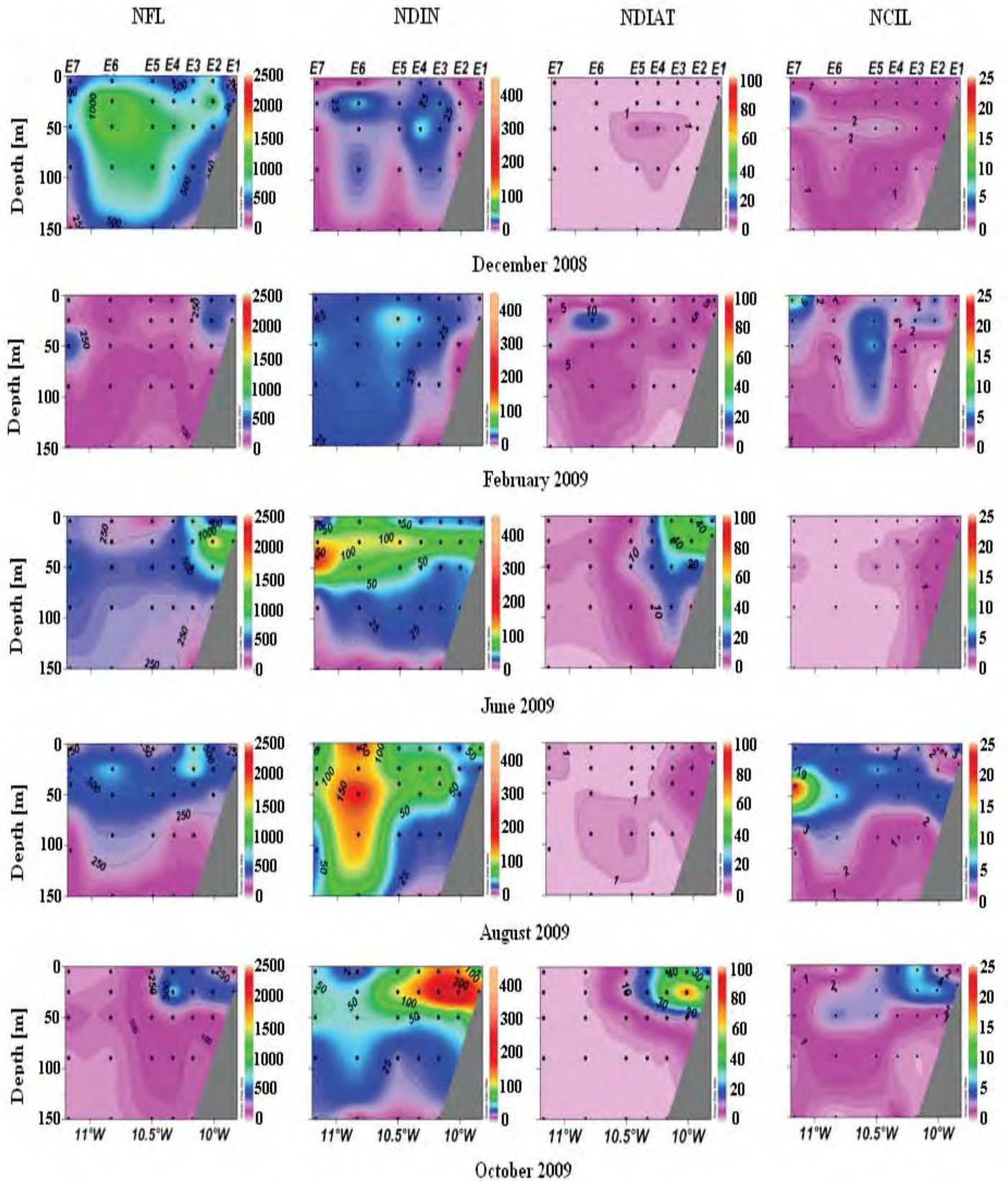


Figure 7

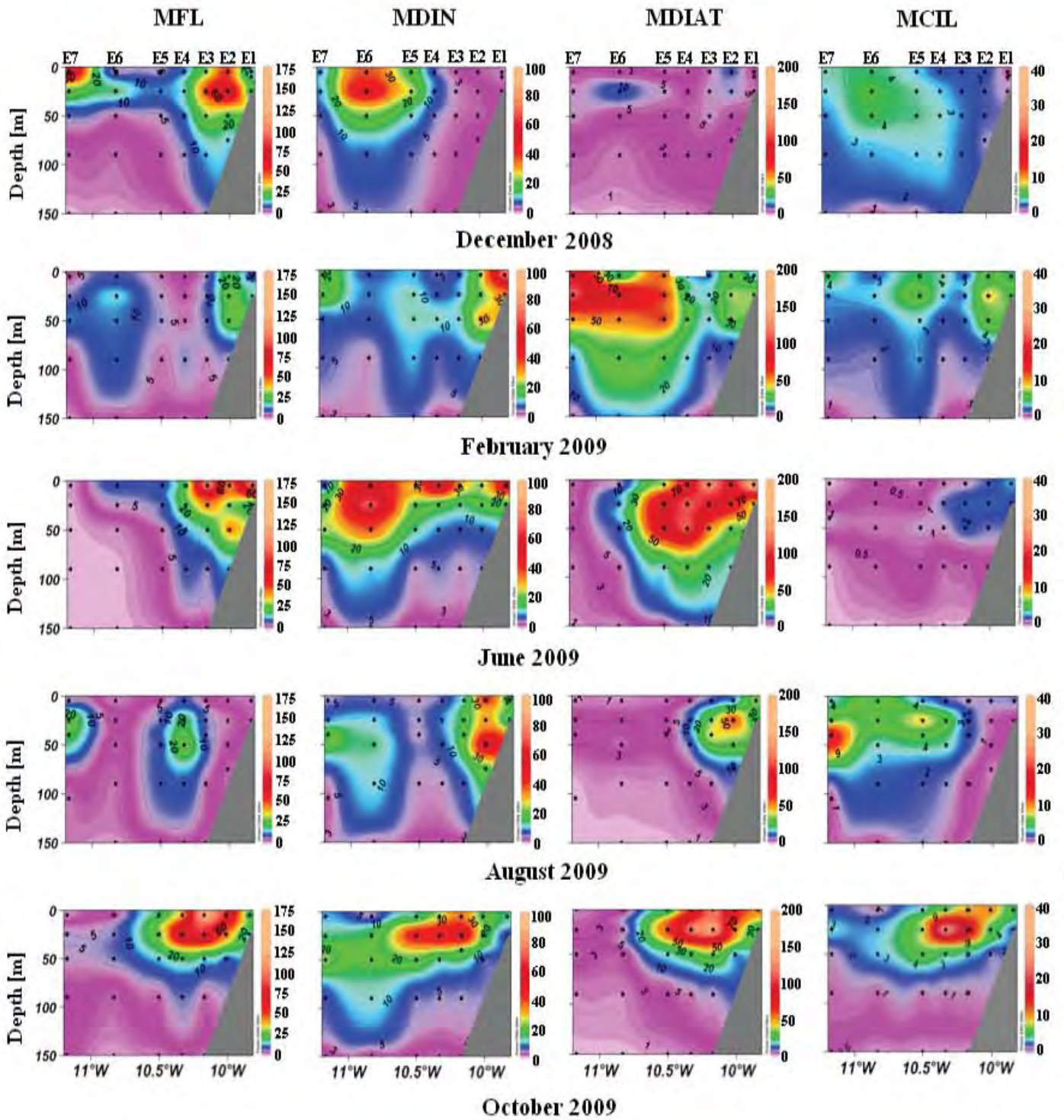


Figura 8

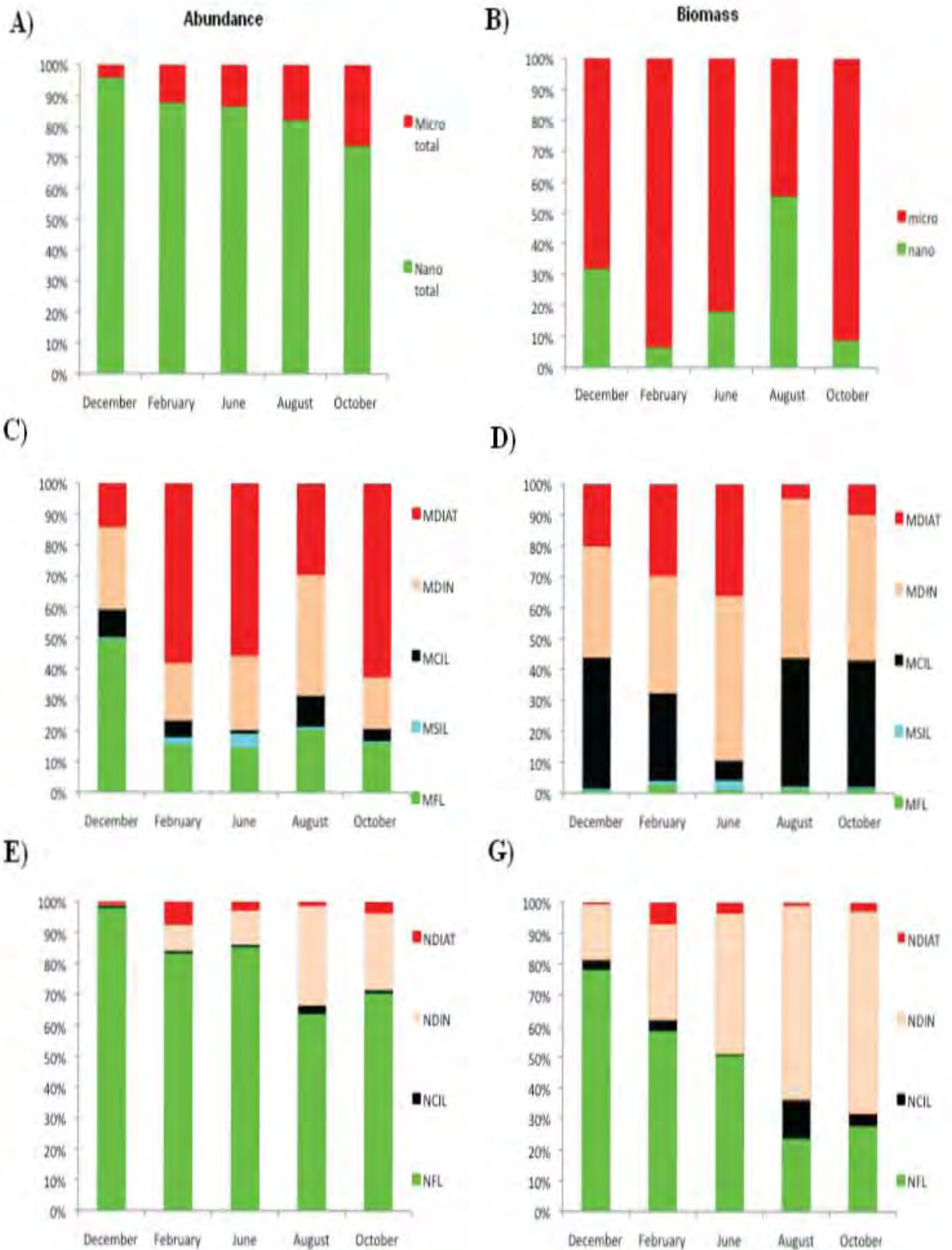


Figure 9

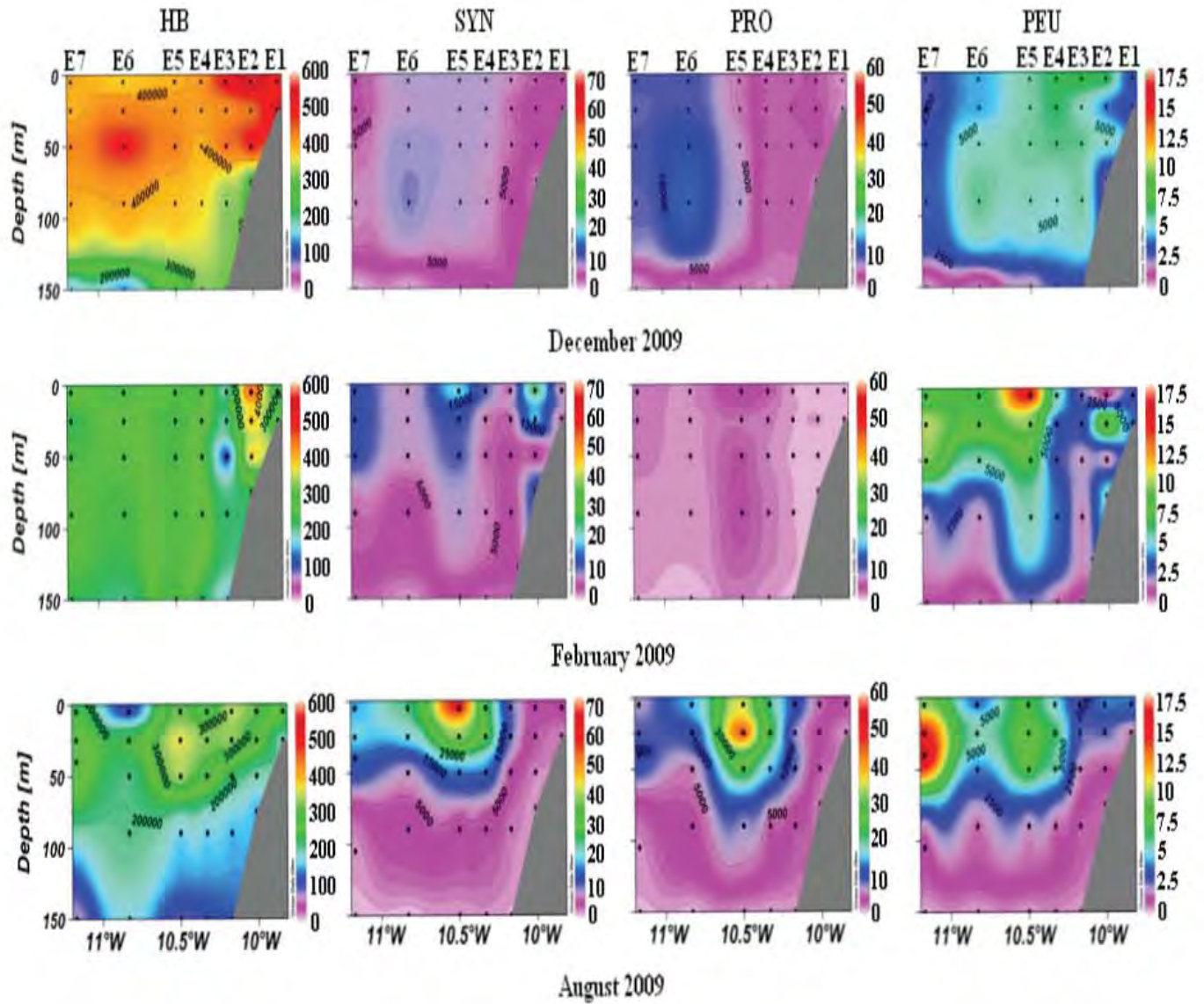
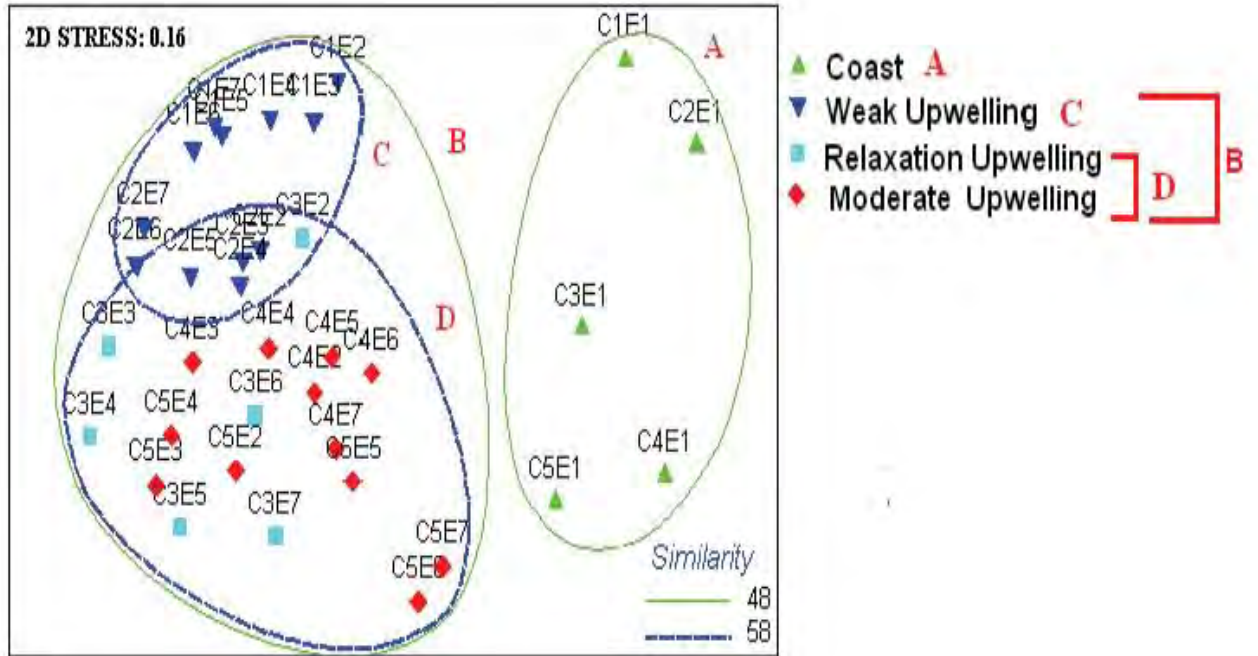


Figura 10

A)



B)

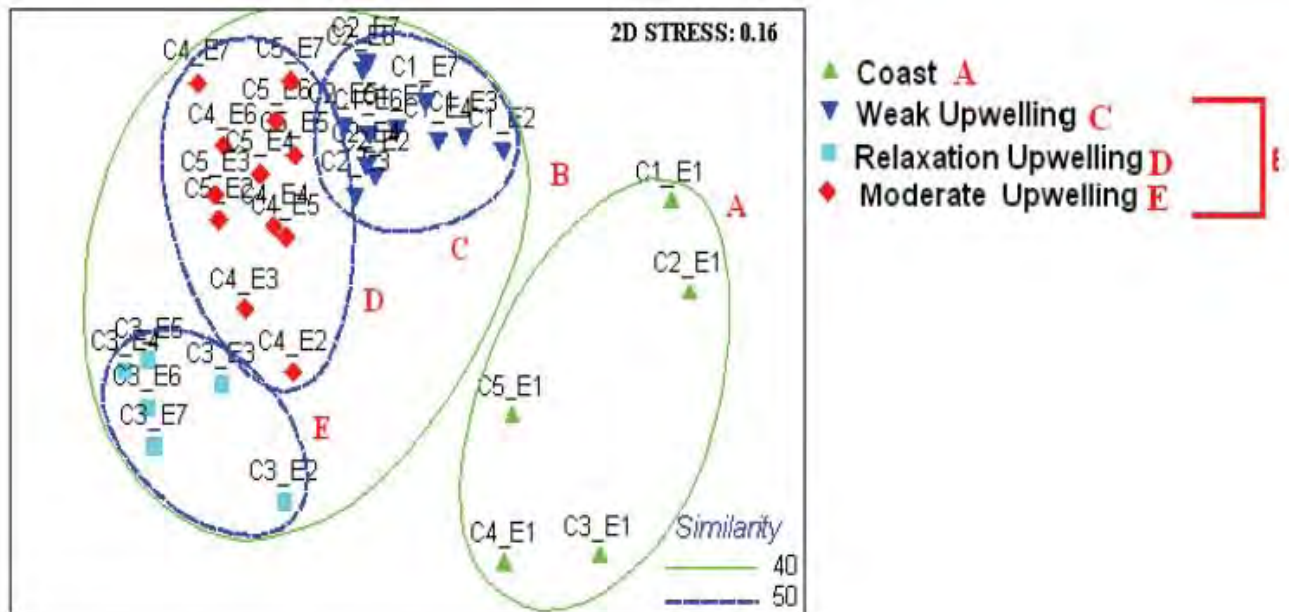


Figure 11

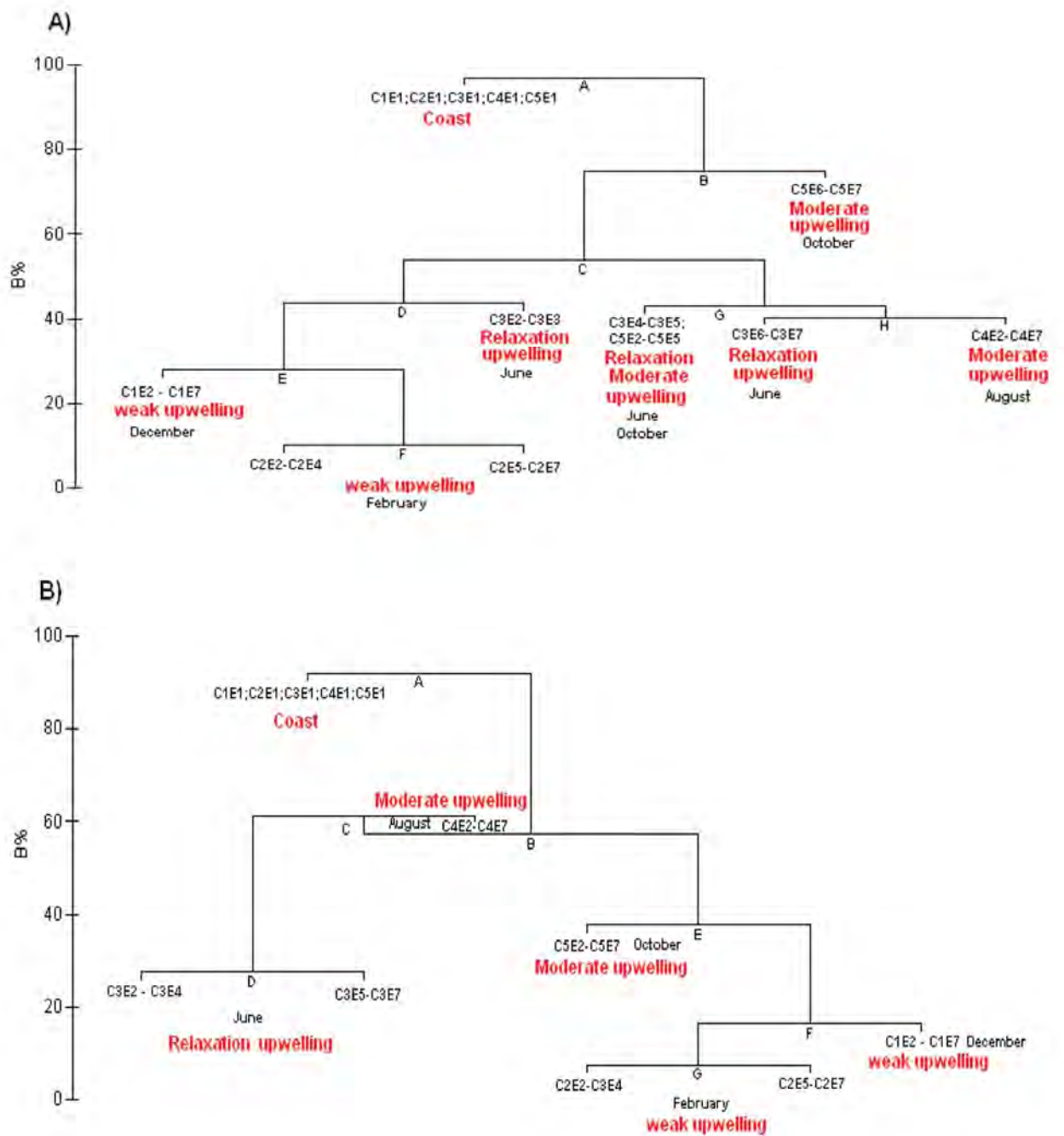
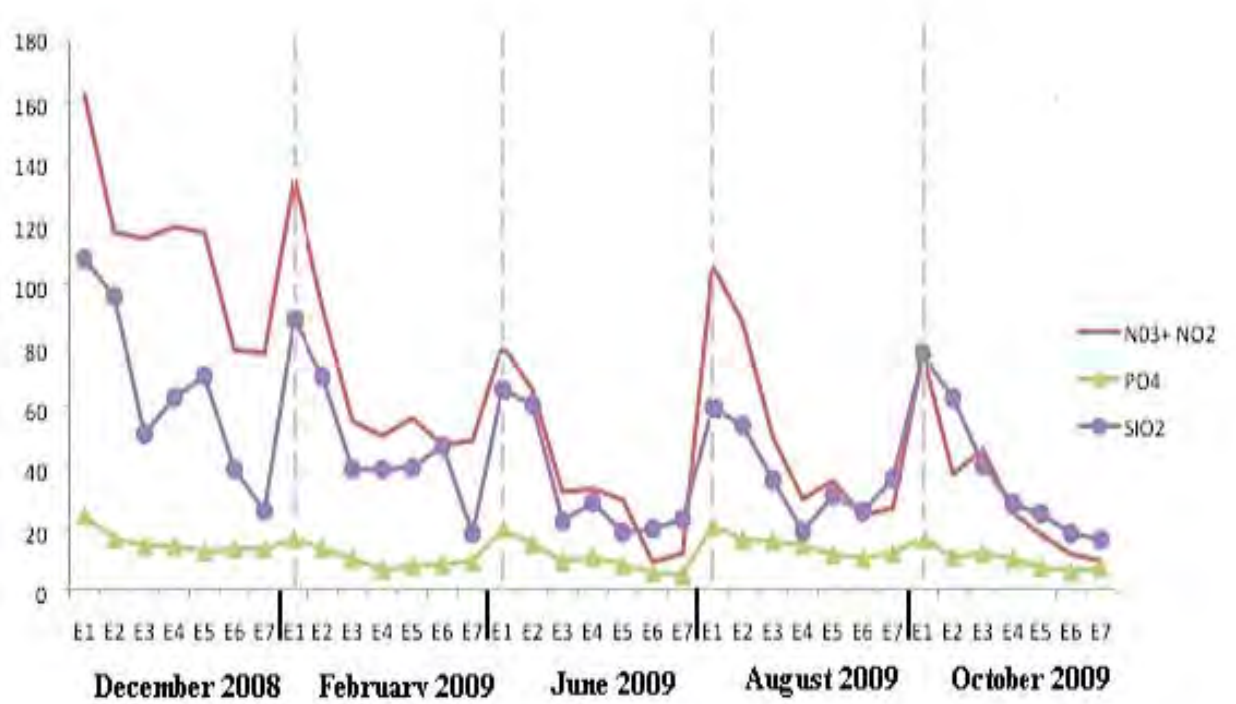


Figure 12



Tables

Table 1. Meteorological and oceanographic conditions during the samplings carried out in the upwelling zone off Cape Ghir (from December 2008 to October 2009). Mean (upper line) and standard deviation (lower line) values for each variable during each sampling time. Satellite-derived data on wind stress (W , $N m^{-2}$), WD correspond to mean values wind stress for 5 days antes y durante and Sea Surface Temperature (SSTs, $^{\circ}C$) correspond to mean values for 5 days (4 prior to and the day of each cruise) in the area between $29.5 - 32.5^{\circ}N$ and $12.5-9.8^{\circ}W$. Other data include: a stability index (\emptyset , $J m^{-3}$) for the upper 150 m water column; in situ SST ($^{\circ}C$); the SST gradient ($^{\circ}C$) along the sampling transect (SSTd); surface salinity (SS); and nutrient concentrations ($mmol m^{-2}$): nitrate (NO_3), nitrite (NO_2), phosphate (PO_4), silicate (SiO_2), Chl-a as total and in size fractions ($mgC m^{-2}$): microplankton (Chl-a M $>20\mu m$), nanoplankton (Chl-a N $20-3\mu m$), and picoplankton (Chl-a P $<3\mu m$) respectively.

samplings	W	WD	SSTs	\emptyset	SST	SSTd	SS	N03	N02	P04	SiO2	Chl-a total	Chl-a M	Chl-a N	Chl-a P
Dec-08(C1)	-0.15	8	16.9	8	16.2	1.7	36.6	690	90	80	300	53	15	31	6
WEUP	0.1		0.09	8	0.6		0.5	320	40	30	160	20	9	15	4
Feb-09 (C2)	-0.06	1	16.7	6	16.5	1.3	36.4	310	90	50	280	56	20	32	5
WEUP	0.04		0.2	4	0.5		0.1	140	50	20	110	25	9	15	4
Jun-09 C3)	-0.1	-2	19.2	71	18	3.5	36.2	380	60	60	270	81	18	58	6
RELAX	0.14		1.3	41	1.7		0.2	150	30	30	120	47	15	60	3
Aug-09 C4)	-0.13	-3	19.3	101	18.5	4	36.6	390	60	70	250	35	4	18	13
MOUP	0.1		0.4	49	1.8		0.5	150	30	30	90	15	4	9	6
Oct-09 (C5)	-0.13	2	20.6	122	19.5	3.9	36.4	340	30	50	280	76	26	44	5
MOUP	0.01		0.6	54	1.6		0.1	140	30	20	110	48	21	53	5

Table 2. Taxa or type composition in the nano- and microplankton size fractions during the samplings off Cape Ghir (December 2008 – October 2009). The components contributing with abundance and biomass >1% of the total are shown. C= carbon content (pg C cell⁻¹); size estimates (in parenthesis) are given only in the cases in which a wide range was observed.

DINOFLAGELLATES	C	DIATOMS	C	DIATOMS	C
Gymnodiniaceae		Chaetocerotaceae		Corethraceae	
Gyrodinium sps (5-11)	25	Bacteriastrium delicatulum (6-20)	140	Corethron sp.	1322
Gyrodinium sps (11-20)	131	Chaetoceros compressus (6-7 x 11-15)	35	Paraliaceae	
Gyrodinium sps (21-40)	1471	Chaetoceros constrictus (14-20 x 15-20)	157	Paralia sulcata	88
Gyrodinium sps (41-60)	3796	Chaetoceros convolutus (15-20 x 20)	163	CILIATES	
Gyrodinium sps (61-95)	7453	Chaetoceros decipiens (11-20 x 11-21)	178	Ascampbelliellidae	
Gyrodinium spirale	3460	Chaetoceros didymus (15-20 x 15-20)	131	Ascampbelliella sp	17624
Gymnodinium sps (6-11)	44	Chaetoceros lauderi	223	Acanthostomella sp	1848
Gymnodinium sps (11-20)	269	Chaetoceros socialis	19	Podophrydae	
Gymnodinium sps (21-40)	842	Rhizosoleniaceae		Podophryra sp	2645
Gymnodinium sps (41-60)	3140	Dactyliosolem fragilissimus	344	Didiniidae	
Gymnodinium sps (61-95)	10303	Guinardia flaccida (25-90)	1443	Didinium sp	9495
Cochlodinium sp.	580	Guinardia striata (6-45)	4089	Halteriidae	
Torodinium robustum	633	Guinardia delicatula (9-30)	358	Halteria sp (21-40)	1138
Katodinium sps (21-40)	557	Rhizosolenia pungens (4-10 x 200-700)	623	Strombidiidae	
Katodinium glaucum (20)	223	Rhizosolenia hebetata (8x 400-500)	682	Tontonia (21-40)	2817
Amphidinium sps (8-20)	374	Rhizosolenia imbricata var. minuta	773	Strombidium sp (41- 115)	8358
Amphidinium sps (21-40)	815	Rhizosolenia setigera (7-10 x 400-450)	855	Strombidium sp (21- 40)	2419
Calciodinellaceae		Proboscia alata (2.5-10 x 300-500)	561	Strombidium sp (11-20)	275
Scrippsiella sp. (15-20)	638	Skeletonemaceae		Strombidium sp (5 - 10)	64
Scrippsiella sp. (21-29)	1374	Detonula pumila (16-26)	272	Laboea (45 -115)	7087
Prorocentraceae		Bacillariaceae		Tetrahyemidae	
Prorocentrum gracile	1152	Fragilariopsis doliolus (30-70)	54	Tetrahyena	4825
Prorocentrum micans	2074	Cylindrotheca closterium	23	Mesodiniidae	
Prorocentrum lima	5275	Cylindrotheca longissima	106	Mesodinium sp (21-35)	3015
Prorocentrum minimum	271	Pseudo-nitzschia sp. (3 x 10-40)	14	Mesodinium sp(19- 20)	872
Peridiniaceae		Pseudo-nitzschia pseudodelicatissima	23	Strobiliidae	
Heterocapsa sp. (11-20)	107	Pseudo-nitzschia delicatissima	20	Strobilidium sp	8983
Oxytoxaceae		Pseudo-nitzschia cuspidata (30-80)	30	Tintinnopsis sp	8945
Oxytoxum sp.	2553	Pseudo-nitzschia lineola (56-112)	79	Codonaria sp	18754
Protoperidiniaceae		Pseudo-nitzschia frauenfeldi	164	Undellidae	
Protoperidinium brevipes	2012	Pseudo-nitzschia fraudulenta	113	Undella sp	30193
Protoperidinium bipes	518	Nitzschia sp.	251	Strombidinopsidae	
Protoperidinium conicum	7526	Naviculaceae		Strombidinopsis sp	12190
Protoperidinium oblongum	6706	Navicula directa (50-120)	538	Tintinnidae	
Protoperidinium steinii	2523	Navicula transitans var. deresa (35)	62	Eutintinnus sp	15995
Protoperidinium ovatum	6902	Navicula delicatula (15-49)	30	Salpingacantha sp	4276
Protoperidinium sp. (>45)	2935	Haslea wawriake (70-160)	359	Dadayella sp	2962
Dinophysiaceae		Pleurosigma normanii (90-200)	164	Dictyocystidae	
Dinophysis schroederi	9232	Pleurosigma directa (180-220)	1296	Dictyocysta sp	11440
Dinophysis caudata (50-60)	5370	Meuniera membranacea	56	FLAGELLATES	
Metaphalocroma	613	Diploneis sp.	331	FL (2-6) oval	5
Ceratiaceae		Leptocylindraceae		FL (6-10) oval	71
Ceratium candelabrum	5370	Leptocylindrus danicus	112	FL (11-20) oval	399
Ceratium fusus	3635	Leptocylindrus minimus	23	FL (2-5) pearform	3
Ceratium furca (30-65)	3940	Thalassiosiraceae		FL (6 -10) pearform	15
Ceratium teres	15329	Skeletonema tropicum (4.5-38)	128	FL (11-20) pearforme	166
Gonyaulacaceae		Thalassiosira sp.	1057	Euglenaceae	
Alexandrium sp	1911	Lauderia annulata (24-75)	1046	Euglenofitas sp.	648
Gonyaulax spinifera	3623	Thalassiosira rotula	560	Halosphaeraceae	
Noctilucaceae		Thalassiosira punctigera (40-70)	2155	Pyramimonas sp.	59
Pronoctiluca pelágica	535	Thalassiosira anguste (20-45)	550	Halosphaera sp.	114
Cladopyxidaceae		Thalassiosira minuscula (5-15)	65	Cryptomonadaceae	
Micracanthodinium sp	713	Thalassiosira kushirensis (40-50)	1199	Rhizomonas setigera (4-8)	14
DIATOMS		Thalassiosira subtilis (18)	173	Raphidophyceae	
Fragilariaceae		Thalassionemataceae		Heterosigma sp (15-20)	481
Asterionellopsis glacialis	108	Thalassionema nitzschioides (10-80)	66	Chlorophyceae	
Fragilaria sp. (17)	15	Thalassionema pseudonitzschioides	105	Oocystis sp.	10
Achnantheaceae		Thalassiothrix longissima	1745	SILICOFLAGELLATES	
Achnanthes brevipes	25	Lioloma sp	1064	Dictyochophycean	
Hemiaulaceae		Coscinodiscaceae		Dictyocha fibula	550
Cerataulina pelagica	723	Coscinodiscus wailesii (260-300)	206081	Dictyocha speculum	770
Hemiaulus hauckii (12-35)	334	Coscinodiscus argus (31-110)	4854		

Table 3. Mean and SD of the abundance (ABU, 10^9 cells m^{-2}), biomass (BIO, mg C m^{-2}) of the plankton (size and functional groups) in the water column (0-150 m depth) during each sampling (December 2008- October 2009) in the upwelling zone off Cape Ghir. HB= bacterioplankton, SYN= Synechococcus, PRO= Prochlorococcus, PEU= Picophytoeukaryotes, NFL= Nanoflagellates, MFL= Microflagellates, MSIL= Microsilicoflagellates, MCIL= Microciliates, NCIL= Nanociliates, MDIN= Microdinoflagellates, NDIN= Nanodino­flagellates, MDIAT= Microdiatoms, NDIAT= Nanodiatoms. Mean and SD of the biomass considering mixotrophy (BIOX, mg C m^{-2}) of the organisms (functional groups). HB= bacterioplankton, CIAN= autotrophic bacteria (SYN, PRO), PEU= autotrophic Picophytoeukaryotes, AFL= autotrophic flagellates, HFL= heterotrophic flagellates, ACIL= autotrophic Ciliates, HCIL= heterotrophic Ciliates, ADIN= autotrophic Dinoflagellates, HDIN= Heterotrophic dinoflagellates; DIAT=diatoms. Community descriptors (ratios) and relationships between the planktonic components. Biomass (mgC m^{-2}) autotrophic y heterotrophic functional groups; Hm: heterotrophic total with mixotrophic, Am: autotrophic total with mixotrophic and H:heterotrophic total, A: autotrophic total

Date	ABU	HB	SYN	PRO	PEU	NFL	MFL	MSIL	MCIL	NCIL	MDN	NDIN	MDIAT	NDIAT
DiC-09 (C1)	Mean	47508	677	531	548	55.6	2.22	0.04	0.29	0.15	0.68	1.16	0.37	0.13
WEUP	SD	17560	344	462	261	30.5	1.83	0.02	0.15	0.07	0.52	1.07	0.11	0.08
Feb-09 (C2)	Mean	29071	747	119	451	25.7	0.9	0.06	0.39	0.23	1.05	2.8	3.71	0.71
WEUP	SD	11435	385	91	306	10.5	0.39	0.04	0.19	0.16	0.29	1.52	2.77	0.60
Jun-09 (C3)	Mean					30.7	0.38	0.27	0.09	0.05	1.7	5.49	4.9	0.79
RELAX	SD					14.2	0.4	0.34	0.05	0.03	1.23	3.11	5	0.54
Aug-09 (C4)	Mean	24707	904	881	470	21.5	0.48	0.03	0.35	0.34	2.82	2.83	1.47	0.25
MOUP	SD	9346	742	938	408	7.9	0.55	0.02	0.42	0.22	1.4	1.61	1.04	0.12
Oct-09 (C5)	Mean					11.8	1.84	0.02	0.41	0.21	1.48	5.31	3.55	0.49
MOUP	SD					5.9	1.96	0.03	0.33	0.14	0.63	2.89	3.98	0.42

Date	BIO	HB	SYN	PRO	PEU	NFI	MFI	MSIL	MCIL	NCIL	MDN	NDIN	MDIAT	NDIAT
DiC-09 (C1)	Mean	756	63	15	776	971	144	22	1424	14	1287	179	207	8
WEUP	SD	276	37	14	402	526	21	11	778	8	780	154	140	2
Feb-09 (C2)	Mean	480	75	3	598	745	161	38	1852	18	2039	347	1490	22
WEUP	SD	207	44	3	499	300	98	27	949	15	799	168	821	11
Jun-09 (C3)	Mean					800	60	162	643	3	4286	777	4002	36
RELAX	SD					422	71	200	366	2	3112	476	3949	26
Aug-09 (C4)	Mean	386	96	24	606	412	65	20	1896	23	3573	515	917	15
MOUP	SD	170	100	27	541	204	111	18	2190	14	1657	289	345	10
Oct-09 C5	Mean					297	112	11	2797	20	2603	829	1139	20
MOUP	SD					167	195	15	2207	11	1167	561	667	19

Date	BIOMix	CIAN	PEU	AFL	DIAT	ADIN	ACIL	HB	FHL	HDIN	HCIL	Hm/Am	H/A
Dec-08 (C1)	Average	77	776	950	366	683	356	756	10	783	1082	0.9	1.5
WEUP	SD	46	402	676	181	348	187	276	5	453	588	0.2	0.6
Feb-09 (C2)	Average	78	598	340	1735	981	694	480	35	1406	1175	0.7	1.7
WEUP	SD	46	499	213	870	302	351	207	18	471	557	0.1	0.5
Jun-09 (C3)	Average			1258	4073	1878	427		31	3185	219		
RELAX	SD			593	3985	1410	170		15	2029	84		
Aug-09 (C4)	Average	140	606	396	1139	1391	678	386	50	2697	1242	1	2
MOUP	SD	159	362	228	444	801	719	156	32	1308	1218	0.1	0.9
Oct-09 (C5)	Average			231	1395	1296	1118		22	2137	1699		
MOUP	SD			345	865	498	827		12	923	1263		

Table 4: Percentage of contribution to the dissimilarity in the abundance of taxa/types between the 3 biological cluster groups (A, B, and C) distinguished by cluster and MDS analyses for the nanoplankton and the microplankton size fractions (see Fig. 11a). SIMPER analysis, cut off at 75% accumulated frequency.

Group or Family	Dissimilarity (%)				Representative taxa or types
	A-B	A - BC	A- BD	BC - BD	
NFL 1	11	8	14	8	FLo (2-6) oval
NFL 2	4	4	6	2	FLp(6-11) periforme
NFL 3	4	4	5	3	FLo(6-11) oval
Total NFL	35	22	33	20	
Halosphaeraceae	2	2	3	2	Pyramimonas and others taxas
Cryptomonadaceae	3	2	3	4	Rhizomonas setigera
Chaetocerotaceae	2	3	3	1	Chaetoceros socialis and others taxas
	1	2	1	1	Guinardia delicatula
Rhizosoleniaceae	2	4	3	3	
Leptocylindraceae	2	3	1	3	Leptocylindrus minimus
	1	2	1	2	Navicula transitans
Naviculaceae	2	3	2	2	
	1	2	1	1	Pseudo-nitzschia delicatissima
Bacillariaceae	5	8	7	9	
	1	2	1	2	Thalassiosira rotula
Thalassiosiraceae	4	5	4	4	
	6	6	3	9	Gymnodinium sps (5-40)
	2	2	2	2	Gyrodinium sps (5-20)
Gymnodiniaceae	12	14	11	19	
Prorocentraceae	2	2	1	3	Prorocentrum sps
Peridiniaceae	3	2	1	3	Heterocapsa sps
Ceratiaceae	1	2		3	Ceatium teres rand other taxas
	3	3	2	3	Strombidium sps (5-115)
Strombidiidae	4	3	3	3	
Average	53	43	55	52	
FL	37	57	66	39	
DIAT	28	22	13	17	
DIN	25	15	13	33	
CIL	7	6	6	10	
SIL	3	1	2	1	
Average	58	32	53	43	
HB	3	5	14	11	
APP	6	4	6	8	
PP (APP+HB)	9	9	20	19	
FL	12	28	37	25	
DIAT	15	28	15	17	
DIN	34	23	15	25	
CIL	20	3	3	9	
SIL	1	1	2		
Average	61	34	54	53	

Table 5: Percentage of contribution to the dissimilarity in the biomass of taxa/types between the 4 biological cluster groups (A, B, D, and C) distinguished by cluster and MDS analyses for the nanoplankton and the microplankton size fractions (see Fig. 11b). SIMPER analysis, cut of at 75% accumulated.

Group or Family	Dissimilarity (%)							Taxa or types
	A-B	A-BC	A-BE	A-BD	BC-BD	BC-BE	BE-BD	
NFL3	2	2	1	1	1	2	2	FLo (6-11) oval
NFL4	2	2	1	1	1	1	1	FLp (11-20) periforme
Total NFL	10	10	4	6	3	7	4	
Dictyochophyceae	2	2		1	1	3	2	Dictyocha sps
	4	2	2	2	4	4	4	Guinardia striata
Rhizosoleniaceae	5	5	4	6	6	6	6	
Leptocylindraceae	1		1	1	3	2	3	Leptocylindrus sps
Bacillariaceae	1	1	2	3	1	1	1	Pseudo-nitzschia and others taxas
	1	1	1	1	3	3	3	Thalassiosira rotula
Thalassiosiraceae	5	4	4	5	6	6	6	
Coscinodiscaceae	4	2	5	5	6	7	2	Coscinodiscus sps
	10	10	8	5	5	3	4	Gyrodinium sps (21-90)
	7	3	8	6	3	4	3	Gymnodinium sps (5-40)
Gymnodiniaceae	22	20	23	19	14	12	16	
Protoperidiniaceae	4	3	4	4	5	5	5	Protoperidinium sps
Calciodinellaceae	2	2	3	2	2	2	2	Scrippsiella sp
	2	0	1	1	7	8	6	Ceratium teres
Ceratiaceae	5	2	4	3	11	14	11	
Dinophysiaceae	1	1	1	1	3	3	3	Dinophysis sps.
Oxytoxaceae	2	1	2	1	3	3	3	Oxytoxum sps
	2	1	2	2	2	3	2	Eutintinnus sp.
Tintinnidae	3	2	3	3	3	4	3	
	5	6	5	3	2	2	3	Strombidium sps. (21-115)
	2	2	3	2	1		2	Laboea sp. (45-115)
Strombidiidae	8	13	11	8	6	3	7	
Mesodinnidae	2	2	2	1	2		3	Mesodinium sp.
Hymenostomatida	2	3	2	1	2		1	Tetrahymena sp.
Average	66	63	66	51	60	70	56	
FL	11	21	7	17	8	12	10	
DIN	43	24	31	30	38	37	22	
DIAT	21	16	39	20	20	34	34	
CIL	21	34	16	29	32	10	24	
SIL	4	5	6	4	3	7	8	
Average	66	44	28	21	48	54	25	
	A-B	A-BC	A-BE	BC-BE				
HB	3	5	4	1				
APP	6	6	4	3				
PP (APP+HB)	9	11	8	4				
FL	11	12	7	8				
DIAT	15	15	13	26				
DIN	34	31	44	40				
CIL	21	22	18	16				
SIL	1	2	1	1				
Average	61	61	65	49				

Table 6: Results of the LINKTREE analysis to identify the environmental variables that best explain the separation of the clusters formed by the abundance and biomass of the planktonic components (see clusters in Fig. 12); the corresponding ANOSIM correlation (r) and probability (P) values, and the value(s) which characterize each environmental variable for the clusters compared are also shown.

Cluster Abundance	r-value	P	Variables	Levels
A -B	0.88	$P \leq 0.001$	SiO2	A (<0.1) ; B(>0.14)
			P04	A (<0.04); B (>0.05)
B -C	0.66	$P \leq 0.001$	SST	C (<20.3); B (>21.5)
C-D;G	0.6	$P \leq 0.05$	SST	D (>17.1); G (<17.2)
D-E	0.76	$P \leq 0.001$	SS	E(>36.2); D(<36.1)
			WD	D(>-2); E (< 8)
E-F	0.9	$P \leq 0.001$	WD	F (>5); E (<8)
F	0.74	$P \leq 0.001$	N03	F (<0.4); F (>0.29)
			SS	F (<36.5); F (>36.5)
			SST	A (<16.8); B (>16.8)
G-H	0.81	$P \leq 0.001$	SST	H (<19); G (>19.8)
H	0.95	$P \leq 0.001$	P04	H (<0.06); H (>0.08)
			N03	H (<0.3); H (>0.5)
Cluster Biomass	r-value	P	Variables	Levels
A-B	0.85	$P \leq 0.001$	SiO2	A (<0.09) ; B(>0.14)
			P04	A (<0.04); B (>0.05)
B-C; E	0.62	$P \leq 0.001$	WD	C (<-2); E (>1)
C-D	0.91	$P \leq 0.05$	WD	C (>-3); D (<-2)
D	0.78	$P \leq 0.001$	SS	D (<36.2); D (>36.4)
			SST	D (<17.2); D (>18.6)
			P04	D (>0.085); D (<0.082)
E-F	0.84	$P \leq 0.001$	SST	E (>18.2); F (<17.1)
			N03	E (<0.58); F (>0.55)
F-G	0.84	$P \leq 0.001$	WD	A (<1); B(>8)
G	0.81	$P \leq 0.05$	NO3	G (<0.4); G (>0.3)
			SS	G (<36.5); G (>36.5)
			SST	G(<16.8); G (>16.8)

Tabla 7 Community descriptors (ratios) and relationships between the planktonic components. Biomass (mgC m⁻²) of H: heterotrophic total , A: autotrophic total, H: heterotrophic total corrected , Ac: autotrophic total corrected, HB (heterotrophic bacterioplankton), APP (autotrophic picoplankton), NHT (heterotrophic nanoplankton), NAT (autotrophic nanoplankton), MHT (heterotrophic microplankton), MAT (autotrophic microplankton); H: heterotrophic total , A:

autotrophic total . Chl-a as total and in size fractions: microplankton (Chl-a > 20), nanoplankton (Chl-a 20-3), and picoplankton (Chl-a <3). Chl-a as total and in size fractions: microplankton (Chl-a > 20), nanoplankton (Chl-a 20-3), and picoplankton (Chl-a <3).

Sampling	A: Chl-a total	Ac: Chl-a total	MATc: Chl-a micro	MAT: Chl-a micro	NAT: Chl-a nano	APP: Chl-a pico
Dec-08	50	60	74	30	42	148
Feb-09	50	60	140	100	20	162
Jun-09			390	310	31	
Aug-09	64	80	450	330	75	27
Oct-09			160	90	14	
REGRESSIONS						
All samplings	A: Chl-a total y = 34.875x + 926 R ² = 0.49, p= 0.001	Ac: Chl-a total y = 44.03x + 1122 R ² = 0.58, p= 0.0007	MATc: Chl-a Micro y = 92.539x + 1127 R ² = 0.51, p = 0.05	MAT: Chl-a Micro y = 61.303x + 528.13 R ² = 0.35, p = 0.1	NAT: Chl-a Nano y = 44.916x - 172.32 R ² = 0.60, p=0.0001	APP: Chl-a Pico y = 89.945x + 310.63 R ² = 0.59, p = 0.0001
	H: Chl-a total y = 34.831x + 753 R ² = 0.51, P=0.05	Hc: Chl-a total y = 40.3641x + 1143.1 R ² = 0.51, P=0.05	MHTc: Chl-a total y = 34.713x + 741.6 R ² = 0.51, p=0.003	MHT: Chl-a total y = 46.17x + 1012 R ² = 0.57, p=0.003	HB:NHT y = 0.1588x + 11.46 R ² = 0.47, p=0.003	HB: Chl-a total y = 9.411x + 108.51 R ² = 0.61, p=0.0002